Computer Networks 176 (2020) 107257

Contents lists available at ScienceDirect

Computer Networks

journal homepage: www.elsevier.com/locate/comnet

LiM-AHP-G-C: Life Time Maximizing based on Analytical Hierarchal Process and Genetic Clustering protocol for the Internet of Things environment

Khalid A. Darabkh [a,*], Wafa'a K. Kassab [a], Ala' F. Khalifeh [b]

[a] The University of Jordan, Amman, 11942, Jordan
[b] German Jordanian University, Amman, 11180, Jordan

ARTICLE INFO

Keywords:
IoT environments
Smart city
Routing
Clustering
AHP
Cluster head rotation
Throughput
GA
Broadcast domain
Wireless sensor
IoT communication protocols
Multi-band antennas
FHSS

ABSTRACT

Contemporary smart sensing paradigms, that are provided via diverse Internet of Things (IoT) mechanisms, propagate across considerable domains of daily life, such as health, agriculture, transportation, trade sectors to urban environments and smart cities. The new era of revolution in information technology will rely on processing and analyzing big data that are gathered by tremendous numbers of intelligent sensors, which are disseminated in the surrounding regions. However, most of these devices suffer from restrictions on power resources and processing capabilities, which in turn will enforce stringent restrictions on the network operations. In view of this, the development of novel and efficient energy algorithms for IoT paradigm is a challenging issue bearing in mind that the performance of this state-of-the-art network paradigm cannot be handled effectively by the existing techniques or solutions that are utilized in wireless sensor networks. To meet the requirements of maximizing the IoT network lifetime, we address in this work the challenge of IoT networks as of embedding energy-constrained devices by proposing a novel protocol, namely, Life Time Maximizing Based on Analytical Hierarchal Process and Genetic Clustering (LiM-AHP-G-C) protocol. In particular, the proposed protocol presents a novel optimal clustering algorithm for un-rechargeable battery-powered IoT devices, an efficient IoT heads selection algorithm, a heuristic method for optimal hop selection, and a model for avoiding intra- and inter-cluster interferences for IoT networks. The simulation results show that our proposed protocol outperforms the other existing works in terms of network lifetime, resource utilization, and scalability metrics.

1. Introduction

The Internet of Things (IoT) term was first coined by Kevin Ashton in 1999, to belong later to the fundamental block for the upcoming intelligent world that paves the way to the information revolution era [1,2]. In specific, the IoT technology builds a bridge between the cyber domain and the things inside the physical world to permit unprecedented ubiquitous surveillance and intelligent control. The major idea behind IoT is that in the close future, most of the things that surround us will be accessible, sensed and connected inside the dynamic, living, global structure of the Internet [3]. Wireless Sensor Network (WSN) plays a considerable role in IoT as of covering a spacious application range indispensable for the IoT. The IoT networks are similar to WSNs, where the nodes in both networks are battery-powered microsystems embedded with transducers to monitor the surrounding [4]. However, the IoT nodes are embedded with a wireless radio to form a wireless network autonomously and communicate with each other. Nevertheless, these nodes have severe resource constraints in terms of battery power, memory size, computational and communication capabilities [2,5]. These factors should be taken into account as they are deemed as a blueprint for the prosperity of the entire routing process, which requires optimizing the conventional field estimation and data aggregation methods such as multi-hopping and clustering techniques.

1.1. Problem statement

Commonly, prolonging the network lifetime depends on the effective management of the energy resources [6]. In fact, the energy consumption is one of the most critical issues that must be taken into consideration while designing IoT networks. Most generally adopted energy preservation techniques, in the near past, are data aggregation, duty cycling, and clustering [7–9]. Data aggregation approach aims to eliminate any replication in the transmitted data in addition to reduce the number of packets that reach the fog node [10,11]. Duty cycling is an

* Corresponding author.
E-mail addresses: k.darabkeh@ju.edu.jo (K.A. Darabkh), wafaa.kassab@mof.gov.jo (W.K. Kassab), ala.khalifeh@gju.edu.jo (A.F. Khalifeh).

https://doi.org/10.1016/j.comnet.2020.107257
Received 1 December 2019; Received in revised form 5 April 2020; Accepted 8 April 2020
Available online 12 May 2020

operational method that is utilized to minify the amount of energy consumption caused by sensor nodes, while being in the idle mode, through periodically placing them in the sleep mode, thereby lowering the duty cycling (i.e., having more power-saving) [12,13]. The fog computing paradigm is proposed to extend cloud computing services from the core to the edge of IoT networks as of providing a highly virtualized platform that supplies many networking, storage and computational services between smart devices and cloud computing. On the other hand, clustering techniques rotate the different roles among smart nodes to preserve energy and ameliorate the network scalability through reducing packet collisions and channel contentions, which will certainly improve the throughput of the IoT network [14–16]. Unfortunately, the Cluster Head (CH) role in the previous works rises a heavy burden on the CHs, which results in depleting their energy faster than other cluster nodes. Thus, when the CH node dies, no communication can take place in that cluster. The IoT clusters with similar node's density and coverage area have nearly the same amount of intra-cluster communication traffic. However, the traffic from far away cluster heads require to be relayed by other heads closer to the fog node. Based on that, the CHs that are located closer to the fog node exhaust their energy faster than other heads, causing the energy hole problem. Hence, one critical matter that emerges in such energy-constrained IoT networks, is how to avoid the energy hole for the reason of enhancing the network lifetime. Furthermore, in the IoT network, the sensed data messages are transmitted in either an event-driven or a continuous way, which requires employing efficient energy preservation techniques for maintaining the energy of these nodes. Green networking mechanisms also play a remarkable role in IoT networks in order to reduce the energy exhaustion and pollution [4].

1.2. Methodology and contributions

As an alternative to the existing IoT network paradigms, we develop a novel lifetime maximization network model that aims at mitigating the long-distance communications, especially, in the smart city environment, when the number of smart sensors exceeds hundreds or thousands. Actually, the round-based policy, which is set by the central control like fog node, is the best clustering-based time-division policy, considered for evaluating the performance of WSNs environment, in which the setup and steady-state (data transmission) stages are involved. The setup stage, which is also known as the offline stage, is the most complicated and crucial fissure in which the network configurations, that are required for the operation of the IoT network, are set. In our proposed protocol, this phase is performed only once by the fog node before the beginning of the data transmission stage (i.e., transmitting cluster nodes' data), allowing the operation in a proactive and centralized mode. Besides, the main responsibilities, which lie over the fog node in the setup stage, include cluster formation, cluster heads selection, and relaying node nomination per round, which result in curtailing the amount of control overhead that will be induced by IoT sensor nodes when building up clusters. What mainly distinguishes this work from other related works is that the smart sensors are allowed to sense and transmit data utilizing the whole round time (i.e, without deducting part of it for the offline stage) and further without any interference as of being equipped with multi-band antennas, and hence avoiding the possibility of signal interference.

It is worth mentioning that one of the most efficient mechanisms that is utilized to extend the lifetime of IoTs network is the clustering technique [17,18]. Correspondingly, we propose a novel energy-aware clustering and routing protocol that aims at providing easiness in data aggregation, route discovery, and minifying the control overhead required for having proper communications. In particular, our proposed protocol partitions the IoT network area into layers where these layers are split further into equal size clusters, in which the farthest distance between two nodes does not exceed the threshold distance at which the channel propagation models change, thereby keeping the intra-cluster communication process under the use of the Friis free space channel propagation model. Not only to this extent but rather, every cluster in our network model has two heads, namely, CH and leader head (LH) nodes. The LH node is in charge of receiving sensed data from the cluster members to be then aggregated, compressed and subsequently transmitted to its CH. Additionally, the CH node has the duty of sending this data directly to the fog node or relaying it via an appropriate LH node in another cluster, based on how far it is from the fog node. Furthermore, we propose a novel approach for heads selection utilizing Analytical Hierarchical Processing (AHP) algorithm that incorporates multiple interesting parameters, while electing optimal heads to work for a batch of rounds, which include nodes' energy, how far the nodes are from the fog node, and how far the nodes are of each other.

Forwarding the sensed data utilizing the inter-communication state may require one-hop or multi-hop transmissions. The former type is suitable when the distance between the source node and fog node does not override the threshold distance, while the latter is fit for a large-scale network to maintain the communications over Friis free space channel propagation model and provide more scalability, as with the assistance of relaying nodes, the sensed data can be sent to the distant fog node without depleting much nodes' energy. We do not stop to this extent, but rather, we apply a heuristic Genetic Algorithm (GA) for providing the optimal selection of the next-hop, over the energy-constrained IoT network, considering very influential parameters such as the residual energy of the candidate relay node along with its distances toward both the corresponding CH and fog node. Owing to its abundant power, high processing capabilities, and huge storage, the fog node has further the responsibility of selecting the relay nodes.

The smart city application, which is the case of study in this work, consists of different heterogeneous sensors with different capabilities, out of which the sensing range, communication protocols, processing and computation abilities, for the reason of providing various sensing services (i.e., smart parking, smart street lighting, smart traffic light, controlling traffic congestion, air quality management, waste management, structural health building). Consequently, it will be of great interest to be closer to reality as much as possible as the prior proposed assumptions are no longer valid. In other words, it is so imperative to deploy various sensors types utilizing different distributions as the way they should be in practice, hereby maintaining a satisfying and practical performance, high coverage range, and low cost. However, in part of this work has been accepted in [19].

In light of the above, the major contributions of this paper are summarized below:

a) Considering a live smart borough and consequently deploying heterogeneous sensors with different capabilities utilizing Google Earth Pro App in which an OSM file is generated (i.e., exported) for identifying the coordinates of all streets and buildings, in this smart borough, to be then imported into AutoCAD App after being converted into KMZ format. Thereafter, all generated XLS files, from AutoCAD App, are to be imported into Matlab whereas all necessary coordinates are acquired, and the simulation process begins taking into consideration the employment of quite relevant nodes distributions and communication protocols.
b) Proposing a network model that aims at minifying the long-distance communications for the reason of maximizing the IoT network lifetime.
c) Proposing a novel AHP algorithm for selecting the heads, namely, CH and LH (or CL) for each cluster in the IoT network.
d) Proposing a novel genetic algorithm for selecting the optimal relay node for each cluster along with introducing a mathematical expression for describing the best number of relay nodes required for each cluster in the IoT network.
e) Conducting a massive number of simulation experiments for evaluating the performance of the proposed protocol besides implementing the closely related protocols and consequently conduct-

ing comprehensive comparisons in the perspectives of energy efficiency and utilization.

The rest of this paper is organized as follows: In Section 2, prior works, related to maximizing the lifetime of WSNs, are discussed. Section 3 illustrates extensively the proposed protocol. Section 4 presents thorough discussions for the simulation results of the proposed protocol and those directly connected works under the consideration of various scenarios. Finally, concluding remarks and future directions are summarized in Section 5.

2. Related works

In the past decade, diverse clustering techniques were developed to optimize the energy consumption in wireless resource-constrained sensors, where most of the suggested mechanisms belong to the WSNs model. Comparable to WSNs, sensors in IoT networks play a significant role in sensing, collecting, transmitting and receiving data. Thus, in this work, the majority of the issues regarding clustering methods in WSNs model are inherited in the IoT model as well. Interestingly, the WSN lifespan enlargement has been examined in many researches from different points of view, where it is considered to be one of the focal metrics that evaluate the performance of WSN protocols [20–22]. In particular, one of the dominant clustering protocols, that inspires a large portion of WSNs and IoT researchers' community, is the Low Energy Adaptive Clustering Hierarchy (LEACH) as reported in [22], where the sensors, i.e CHs, and ordinary nodes, are grouped into clusters. As CH nodes consume more energy compared with other members, their role will be rotated periodically among sensors in order to evenly distribute the energy consumption. Actually, the LEACH protocol aims to improve the network lifetime in terms of making the First-node-to-die (FND) metric be launched as late as possible. Despite that, this protocol has numerous limitations that resist achieving its objective, such as being unscalable in the large network area. This is due to the fact that all CHs in the LEACH protocol communicate directly with the sink node, which will compel the CHs, that are far away from the fog node, to exhaust their energy faster than those that are closer, which leads to reducing the network lifespan especially in term of FND metric. Moreover, the CH selection process is performed randomly which does not ensure choosing suitable nodes (in terms of their placements and count) to play the heads' role in each round. Finally, choosing the CHs per round will flood the network with control packets which will not only put a hefty burden on the channel bandwidth, but also increase the amount of energy needed to transmit data packets which certainly give rise to minifying the network utilization.

To cope with the LEACH limitations, a centralized version of LEACH, called LEACH-C protocol, was proposed as reported in [17]. The main idea of this protocol is to make the responsibility of CHs selection, in every round, rely on the sink node based on certain dimensions such as the residual energy and coordinates of each node, which are acquired from the control packets that are transmitted by member nodes. Nonetheless, the LEACH-C protocol overwhelms the network with a massive number of control packets sent in every round by all nodes directly toward the sink node. Consequently, an improved version named the Fixed Low Energy Adaptive Clustering Hierarchy (LEACH-F) protocol was developed. In other words, the setup stage overhead is substantially reduced [17,22]. In the LEACH-F protocol, the sink node floods the network with a list of ordered cluster nodes in the first round only. From this list, each node clearly knows its cluster-ID and other member nodes in its cluster so that the first node, appears in this list of that cluster, will serve as a CH in this round and the next one, shown in the list that belongs to the same cluster, will serve as a CH for the next round and so forth, thereby balancing the energy consumption and mitigating the control overhead. One of the major constraints of this protocol is that no criterion was proposed to handle the re-clustering process. Furthermore, this protocol lacks the support of WSN scalability due to its inability of adding or removing nodes once the clusters are set. In addition, it cannot handle the node's mobility. It is good to mention that, in this work, the fog node and sink node are used interchangeably.

The Energy-Balancing Clustering Approach for Gradient-based (EBCAG) routing protocol was introduced in [23]. This protocol constructs an unequal size of network clusters in a ring-based way, neglecting the nodes that belong to the first ring which results in having improper load distribution among nodes. In fact, nodes in the first ring communicate directly with the sink node. Moreover, the EBCAG protocol considers the minimum number of hops to route data toward the sink node through the utilization of a gradient technique.

The authors in [24], proposed the energy efficiency-based improved LEACH protocol to reduce the number of packets that are exchanged between CH nodes and their cluster members. Actually, the sink node selects CH nodes based on their residual energy per round which in turn minimizes the consumed energy and extends the network lifetime. The Energy-Efficient Clustering Using a Round-Robin (RRCH) protocol, which was proposed in [25], considers that after partitioning the network area into clusters, the CH role will rotate in a round-robin fashion to avoid repetitive setup stages, which are considered in the LEACH protocol. In order to improve energy efficiency, this protocol performs a load balancing technique between sensors within the same cluster in the initial setup stage. The threshold-based LEACH protocol was proposed in [26] for the reason of reducing the number of CH reselection procedures. In other words, the CH nodes will stay in their role until their energy levels drop under a specific value. The authors in [27] proposed an improved LEACH routing communication protocol in which a new head role takes over the CH role (i.e., vice CH) in the last periods of each round. As claimed, the idea of using vice CH enlarges the network lifespan, prolongs the period of the steady-state stage, and reduces the frequency of re-clustering operations.

The most related works to our proposed protocol are those introduced in [20,28,29]. In [20], the Constructing Optimal Clustering Architecture (COCA) protocol was suggested in which an optimum cluster-based architecture that aims at improving the overall energy consumption and prolongs network lifespan is constructed. The network area in the COCA protocol is split into identical square layers, which will be partitioned into clusters in a way that the number of clusters increases toward the sink node. Similar to the LEACH protocol, the lifetime of the COCA protocol is divided into rounds, where each round is split into setup and data transmission stages. The network formation is performed at the setup stage while the process of data sensing, aggregation, and transmission are performed in the data transmission stage. Nevertheless, the COCA protocol has many restrictions that are highlighted as follows. All cluster members, located in the same layer, participate in the CH selection process which in turn floods the network area with control packets and consequently affects the network utilization severely. Additionally, the selection of relaying nodes is proposed to be randomized which certainly brings to choosing those nodes that almost run out of energy.

To improve the WSN lifespan, the Unequal Cluster-based Routing (UCR) protocol was proposed [28]. In the UCR protocol, the network area is partitioned into various cluster sizes which specifically are shortened as soon as approaching the sink node which leads to minimizing the energy consumed via the intra-cluster communication process. For the reason of achieving an efficient node distribution over the network area, a proper way of electing suitable CHs is further introduced. Additionally, in the UCR protocol, a policy of whether to relay the traffic directly to the sink node or via a relaying node is presented. Unfortunately, this protocol has a limitation concerning the way the CHs are selected. In other words, the randomness is considered as one of the selection criteria. In addition, the number of control packets generated is massive which definitely leads to making the network function shorter. In fact, more details will be introduced shortly (i.e., in the results section).

The Efficient and Energy-Aware Clustering and Routing Protocol (EA-CRP) was proposed in [18,29] in which the long-distances communications are mitigated and the energy consumption is balanced which both help in prolonging the WSNs lifetime. In the EA-CRP protocol, the WSN area is partitioned into layers where their widths are reduced toward the sink node, but in return, the number of the clusters is increased. Two heads in each cluster are employed to have efficient load balancing. In specific, one head, named as a leader head, is basically in charge of receiving the sensed data from its member nodes, aggregating it, and subsequently transmitting a compressed packet to its corresponding CH. The other head relays that packet to the next downstream layer until it reaches the sink node. Additionally, an efficient policy for CH selection is proposed in which a weight is given for every member node considering different parameters, where lastly, the node that has the highest weight wins the competition and then becomes a CH. Based on the width and length of each layer, different broadcast ranges are used, thereby reducing long-distance communications.

3. The proposed protocol

To this end, we present a new energy-aware clustering and routing protocol for IoT network, namely, Life Time Maximizing Based on Analytical Hierarchal Process and Genetic Clustering (LiM-AHP-G-C) protocol, which will be extensively detailed in this section. In specific, the main protocol hypotheses are provided in Section 3.1. Section 3.2 illustrates the network topology model while Section 3.3 handles the procedure suggested for dividing the network area. Section 3.4 demonstrates the broadcast algorithm while the procedures used in electing cluster heads and relaying nodes are explained in Sections 3.5 and Section 3.6, respectively. The techniques utilized in avoiding intra- and inter-cluster interferences are discussed in Section 3.7.

3.1. Assumptions

The following assumptions are taken into consideration while designing the LiM-AHP-G-C protocol:

a) The IoT network consists of one fog node and a large number of IoT nodes that are distributed over a rectangular area.
b) The IoT sensors are heterogeneous with different types, functions, frequencies, communication protocols, and processing capabilities.
c) The fog node is situated outside the network area with no restriction on its energy and processing capabilities.
d) The fog node and IoT sensors are stationary.
e) Each IoT node should have a unique ID.
f) Nodes are connected with un-rechargeable batteries and fixed energy.
g) The IoT sensors exchange their data with their LH nodes during the round time.
h) All sensor nodes are aware of their location coordinates and know the fog node and the other nodes' locations via GPS.
i) The energy consumed for the computations, performed by a node, is too small compared with the energy consumed for the data transmissions, thus, it is neglected as considered in [30–34].

3.2. The network model

The smart city application of this work is implemented over a rectangular area of equal cluster sizes as shown in both Figs. 1 and 2. Within each cluster, the nodes transmit their sensed data to their LH during the round time using different frequencies to evade signals interference. Consequently, the LH aggregates its sensed data along with the data sent from cluster members into one fixed message, to be then transmitted to the CH. Based on its distance toward the fog node, the latter transmits the aggregated data either directly to the fog node or relays it to another LH, located in a nearby layer toward the fog node, utilizing the inter-cluster communication mechanism. Similar to the EA-CRP protocol, the network lifetime of our proposed protocol is split into rounds bearing in mind the fog node is in charge of determining the round time. In our proposed protocol, the first round only is reserved for the setup stage, while the entire time of other rounds is fully dedicated to the environment sensing and data transmissions as shown in Fig. 3. In this setup stage, the fog node partitions the network area into virtual layers and clusters and determines the nodes belong to each cluster based on their coordinates. Thereafter, it specifies the heads and relaying nodes (if needed) for each cluster.

3.3. Division of network area

Our major concern is how to connect the width and height of clusters with the threshold distance (i.e., the distance where beyond it, the two-ray channel propagation model is used). In specific, the width and height of clusters should be chosen considering the following constraints:

1. Avoiding the transmissions over the two-ray channel propagation model.
2. Making use of the multi-hop routing algorithm proposed in this work.

It is worth mentioning that avoiding the transmissions over two-ray channel propagation model, keeping the transmissions using Friis free-space channel propagation model, maintains having lower transmit power, thereby prolonging the IoT network lifetime. On the other hand, making the multi-hop routing algorithm proposed in this work feasible, the width of the cluster should be much less than the threshold distance. In light of the above, we want to draw the attention to the point that based on empirical and experimental works, we are eventually able to come up with expressions that describe the division of the network area proposed in this work. Particularly, the height of a cluster is half of its width, while the width of a cluster should not exceed 30% of the threshold distance. In addition, we formulate an expression that relates the network length(L_n)with the cluster length(L_c) to have the number of layers(N_l)in the network area as shown below:

$$N_l = ceil(\frac{\rho}{2}), \tag{1}$$

where:

$$\rho = ceil(\frac{L_n}{L_c}). \tag{2}$$

Moreover, the total number of clusters(N_c) in a network area is represented by:

$$N_c = (2N_l)^2. \tag{3}$$

Interestingly, the number of clusters in a layer (N_{c_l}) is expressed as:

$$N_{c_l} = \delta + \sigma \times (L_{num} - 1), \tag{4}$$

where, $\delta$and σrepresent the coefficients that have been selected experimentally, while their values are listed in Table 2 (i.e., simulation parameters table).L_{num} refers to the layer number.

It cannot be missed out to be mentioned that the severe resource of energy consumption in IoT nodes is communication, which highly depends on the distance between the transmitter and receiver [35]. In our work, we follow the same energy radio and channel propagation models that are adopted in [36–38]. Similar to its counterparts [20,28,29], the LiM-AHP-G-C protocol, considers that a LH consumes$E_{DA}(\frac{nJ}{bit}/signal)$for data aggregation process and compression of multiple data messages of length q-bit each, which are those received from its cluster members along with its own message, into one single message to be sent afterward to its CH node. Ultimately, the CH node aggregates that compressed message along with its own data message and consequently transmits a compressed version toward the fog node.

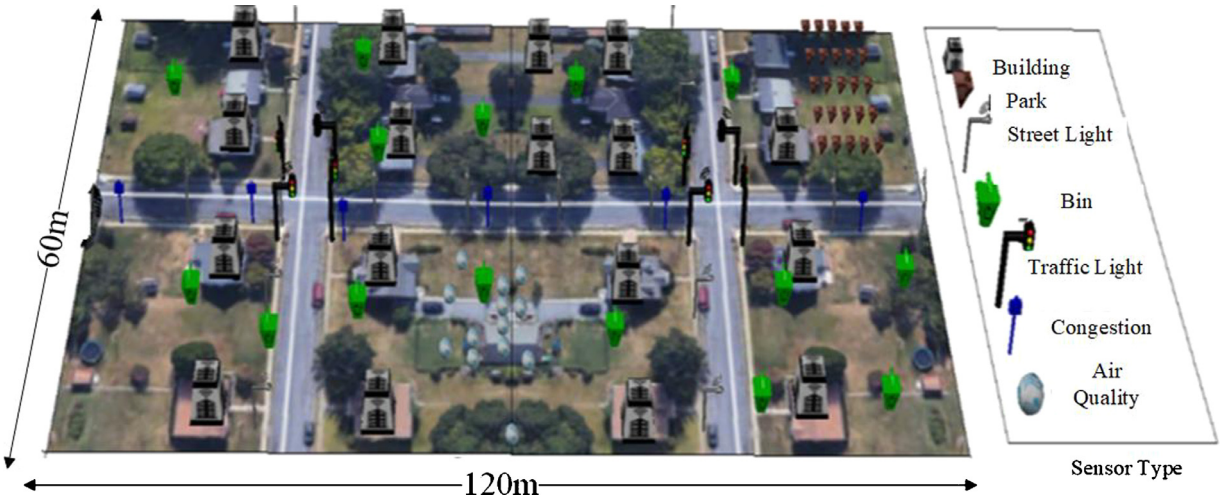

Fig. 1. A 60 x120 IoT area from google earth.

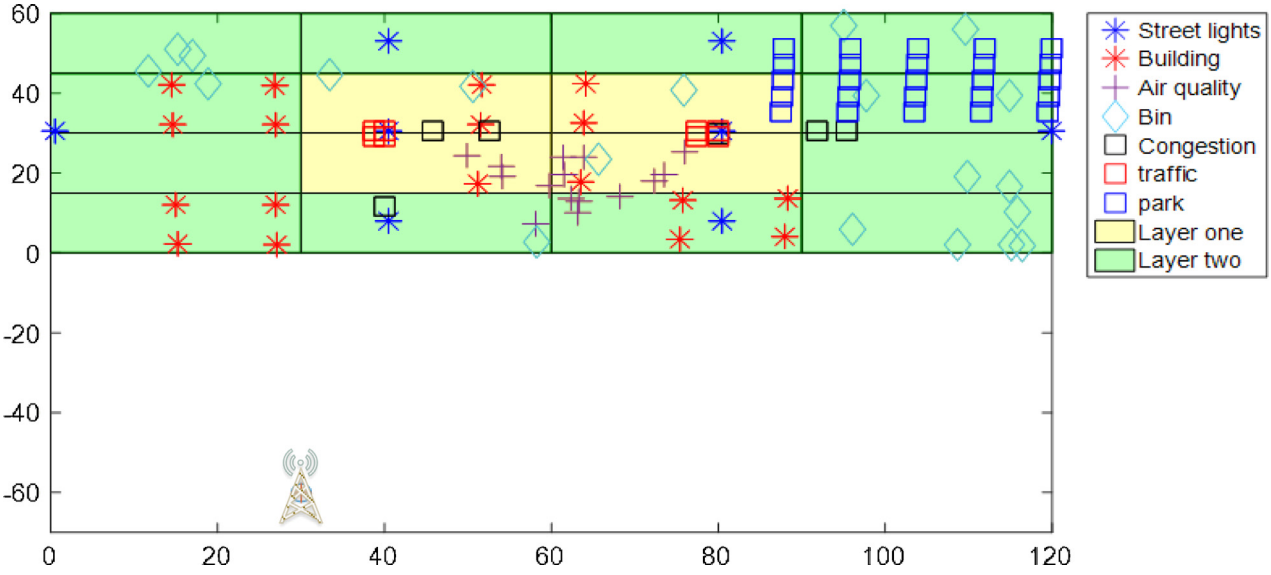

Fig. 2. IoT network model in MATLAB.

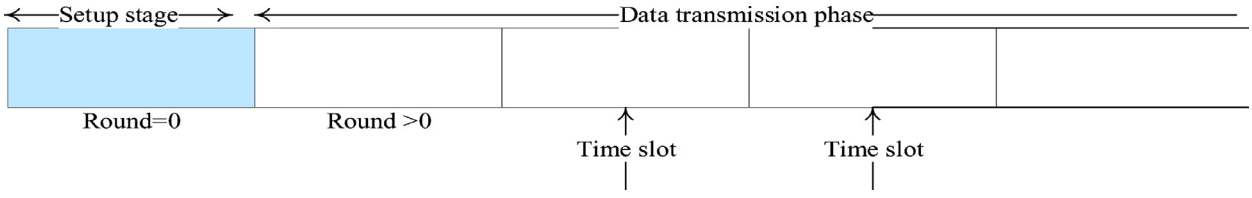

Fig. 3. The division of IoT network lifetime.

3.4. The broadcast algorithm

In the evolving telecommunication world, the multi-band antennas technology has become a desired and significant component for numerous recent communication systems because of their eye-catching properties such as their ability to support multiple bands of frequencies, lightweight, small size, easy fabrication, and low cost [39] [40]. To take advantage of the aforementioned features, we employ such type of antennas in this work, which allows each node to transmit over different frequencies based on its type and the required transmission range, thereby avoiding the intra and inter-cluster communication interferences. Attractively, the fog node is responsible for preparing all the important parameters, required per round, before the beginning of the data transmission stage, such as the layers' ID along with their clusters' IDs, members and heads of each cluster, as well as relay node ID of each cluster (if needed). Consequently, it organizes these parameters into a table to be then broadcasted within the area of its dominance, which allows the nodes further to discover how far they are from it relying on the received signal strength indication. Notably, Fig. 4 shows a portion of a control packet belongs to network clusters of layers 1 and 2 from round 494 to 505.

Round no.	Layer one	Layer two
494	4 clusters	12 clusters
495	4 clusters	12 clusters
496	4 clusters	12 clusters
497	4 clusters	12 clusters
498	4 clusters	12 clusters
499	4 clusters	12 clusters
500	4 clusters	12 clusters
501	4 clusters	12 clusters
502	4 clusters	12 clusters
503	4 clusters	12 clusters
504	4 clusters	12 clusters
505	4 clusters	12 clusters

Cluster no.	Cluster members ID, frequency band and communication protocol								CH ID	LH ID	Relay node for the next hop		
											RN ID	$RN_{x\text{-}cor}$	$RN_{y\text{-}cor}$
1	21	29	32	37	40	57	69	70	29	21	Null	Null	Null
	13.56 MHz	60 MHz	433 MHz	865 MHz	902 MHz	928 MHz	840 MHz	200 MHz					
	RFID	Telensa	Telensa	RFID	RFID	RFID	RFID	Telensa					
2	22	30	31	34	35	36	38	46	73	74	30	38	Null	Null	Null
	200 MHz	869 MHz	60 MHz	13.56 MHz	125 kHz	125.5 kHz	915 MHz	91 MHz	200 kHz	911 MHz					
	Telensa	SigFox	Telensa	RFID	RFID	RFID	Telensa	RFID	SigFox	RFID					
3	3	24	26	72	75	76	81	86	72	3	9	15.186	2.217		
	60 MHz	3.75 kHz	200 kHz	915 MHz	180 kHz	869 MHz	470 MHz	15 kHz					
	Telensa	NB-IoT	NB-IoT	LoRaWAN	NB-IoT	LoRaWAN	Telensa	NB-IoT					
4	2	23	25	66	53	44	68	71	44	2	Null	Null	Null		
	600 MHz	605 MHz	433 MHz	470 MHz	200 MHz	750 MHz	905 MHz	920 MHz					
	SigFox	SigFox	Telensa	Telensa	Telensa	SigFox	RFID	RFID					

Cluster no.	Cluster members ID, frequency band and communication protocol								CH ID	LH ID	Relay node for the next hop		
											RN ID	$RN_{x\text{-}cor}$	$RN_{y\text{-}cor}$
1	9	10	11	12	39	41	43	51	10	9	Null	Null	Null
	60 MHz	916 MHz	200 MHz	865 MHz	433MHz	100 Hz	868 MHz	915 MHz					
	Telensa	LoRaWAN	Telensa	LoRaWAN	Telensa	LoRaWAN	Telensa	Telensa					
2	5	58	33	77	78	79	80	82	95	94	5	33	Null	Null	Null
	905 MHz	200 kHz	190 kHz	193 kHz	195 kHz	60 MHz	433 MHz	64 MHz	203 kHz	868 MHz					
	RFID	NB-IoT	NB-IoT	NB-IoT	NB-IoT	Telensa	Telensa	RFID	SigFox	Telensa					
3	7	17	18	19	20	27	28	67	19	67	Null	Null	Null		
	60 MHz	66 MHz	69 MHz	200 MHz	433MHz	70 MHz	470 MHz	85 MHz					
	RFID	RFID	RFID	Telensa	Telensa	RFID	Telensa	RFID					
4	Null								Null	Null	Null	Null	Null
5	49	61	54	56	59	60	90		61	49	9	15.186	2.217		
	911 MHz	910 MHz	913 MHz	914 MHz	910.5 MHz	909 MHz	920 MHz						
	SigFox	SigFox	SigFox	SigFox	SigFox	SigFox	SigFox						
6	4	48	83	84	85	87	88	89	83	84	9	15.186	2.217		
	869.7 MHz	869.8 MHz	869.5 MHz	870 MHz	871 MHz	872 MHz	873 MHz	874 MHz					
	SigFox	SigFox	SigFox	SigFox	SigFox	SigFox	SigFox	SigFox					
7	42	92	93	97	98	99	100		99	98	33	58.06	7.363		
	100 Hz	869MHz	915 MHz	60MHz	200 MHz	868 MHz	433 MHz						
	LoRaWAN	LoRaWAN	LoRaWAN	Telensa	Telensa	Telensa	Telensa						

Fig. 4. A portion of control packet broadcasted by fog node at the setup stage.

3.5. AHP heads selection algorithm

In this paper, a novel cluster head and leader head selection scheme, which is based on the AHP algorithm, is performed by the fog node due to having unrestricted power source along with high processing speed and huge storage capabilities. The AHP is an effective approach in dealing with complex decision-making processes as of being able to help the decision-makers to place priorities and select the optimal option through splitting complex choices into a series of pairwise comparisons and finally synthesizing the results [41]. Moreover, the AHP incorporates a valuable method for checking the consistency of the decision maker's assessments, hence, lessening the bias in the decision-making process [42]. In this work, the AHP is utilized to deal with both CH and LH selection through considering the following steps:

Step 1: Structuring hierarchy

The objective of the decision, which is selecting an optimal CH and LH per cluster, is prioritized at the highest level of the hierarchy as shown in Fig. 5. The next level comprises of the decision variable (dimensions), whereas the least level includes all the IoT sensors that need to be assessed (alternatives).

Step 2: Calculating the local-weight vector and consistency check

A local weight refers to the weight of each dimension and accordingly will be as an entry of the local-weight vector. However, the approach of finding the local-weight vector is illustrated below.

a) *Making pairwise comparisons*: In order to compute the weights of distinctive dimensions, the AHP algorithm begins with creating a pairwise comparison matrix$A$as shown below:

$$A = \begin{pmatrix} a_{R_e R_e} & a_{R_e D_{fog}} & a_{R_e AVG_{dis}} \\ a_{D_{fog} R_e} & a_{D_{fog} D_{fog}} & a_{D_{fog} AVG_{dis}} \\ a_{AVG_{dis} R_e} & a_{AVG_{dis} D_{fog}} & a_{AVG_{dis} AVG_{dis}} \end{pmatrix}, \tag{5}$$

Taking into consideration that$A$is$m \times m$matrix, where$m$denotes for the number of the evaluated dimensions which include the residual energy of an IoT node(R_e), the distance between that node and the fog node(D_{fog}), and the average distance between that node and other cluster members(AVG_{dis}). Each entry in the matrix$A$(i.e.,a_{ij}) represents the importance of the i^{th} dimension relative to the j^{th} dimension. For instance, if $a_{ij} > 1$, then the i^{th} dimension will be more important and favorable than the j^{th} dimension. Similarly, if $a_{ij} < 1$, then i^{th} dimension will be less important than the j^{th} dimension, while $a_{ij}=1$ indicates that both i^{th} and j^{th} dimensions have the same importance. Based on the above, the relative importance among the two dimensions (i, j)is determined according to a numerical scale that goes from 1 to 9, as shown in Table A.1 at Appendix A. On the other hand, the exact value of the pairwise comparison matrix that is adopted in our simulations is provided in (A.1), found in Appendix A.

b) *Calculating the local weight vector:* Generally, the local weight vector considering all dimensions can be found as

$$w = \begin{pmatrix} w_{R_e} \\ w_{D_{fog}} \\ w_{AVG_{dis}} \end{pmatrix}, \tag{6}$$

Specifically, the local weight vector of dimension i (w_i) is computed by finding the average of every row in the normalized matrixA_{norm}(from matrix A), which is as

$$w_i = \frac{\sum_{k=1}^{m} \bar{a}_{ik}}{m}, \tag{7}$$

where $\bar{a}_{ij}$is the normalized $a_{ij}$and can be computed as

$$\bar{a}_{ij} = \frac{a_{ij}}{\sum_{k=1}^{m} a_{kj}}. \tag{8}$$

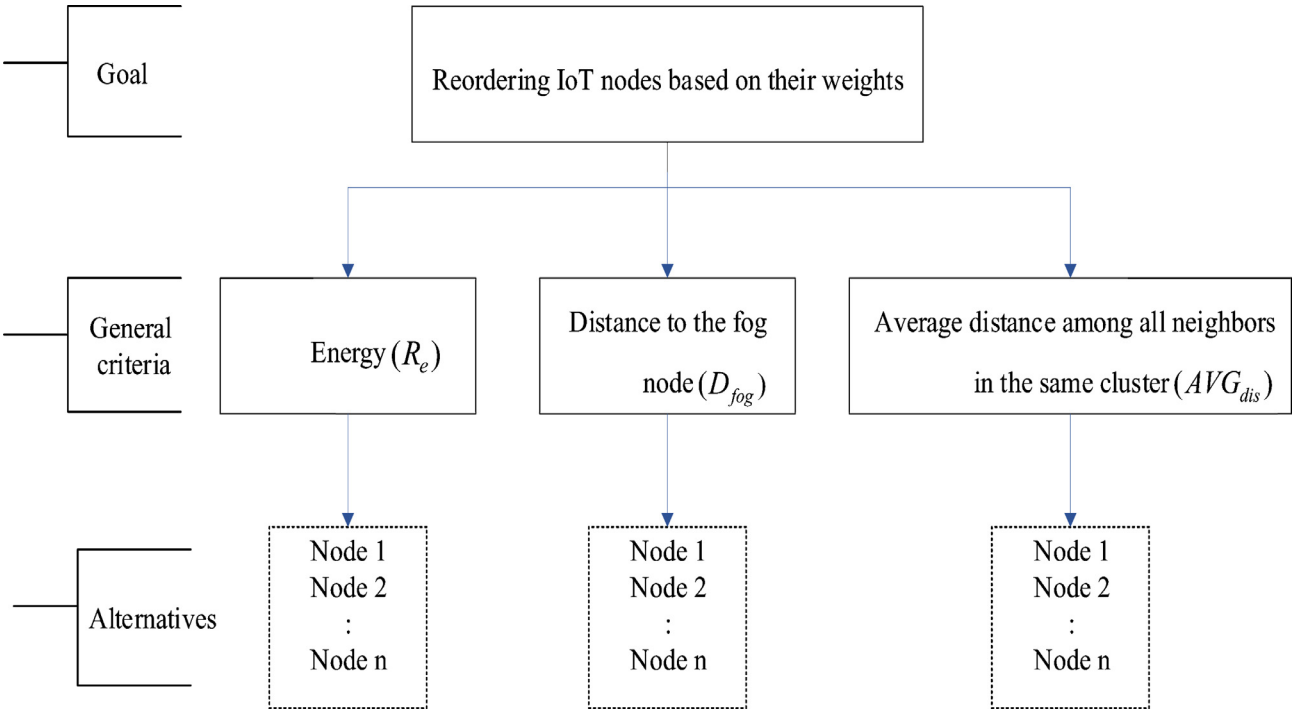

Fig. 5. Structuring AHP hierarchy for CH and LH selections.

It is good to mention that the summation of each column in A_{norm} should be equal to 1.

c) *Checking for consistency:* A matrix$A$ is considered to be consistent as long as $a_{ij} \cdot a_{ji} = 1$. Hence, to check the consistency of any matrix, we should find the Consistency Ratio(CR), which is expressed as

$$CR = \frac{CI}{RI}, \tag{9}$$

where, CIrepresents the consistency index, which is expressed as shown in (10), while RI refers to the random index which can be selected from Table A.2, shown in Appendix A, based on the number of dimensions chosen.

$$CI = \frac{\lambda - m}{m - 1}, \tag{10}$$

where, λ refers to the eigenvalue of the pairwise comparison matrix and is computed as

$$\lambda = \frac{\sum_{k=1}^{m} CO_k}{m}, \tag{11}$$

where, CO represents the consistency vector and can be computed as

$$CO = w_s \times \frac{1}{w}, \tag{12}$$

where, w_s denotes for the weight sums vector and can be calculated as

$$w_s = A \times w. \tag{13}$$

To this end, we can determine whether the comparison matrix is consistent or not based on the following constraint. If $0 \leq CR < 0.1$, then the local weights will be consistent, otherwise, they will be not consistent. If this constraint is not met, then a recalculation is required. In other words, the levels of importance among the three dimensions should be reconsidered to eventually meet this consistency check constraint.

Step 3: Calculating the global-weight vector

The global-weight vector is calculated for each cluster by finding the aforementioned three dimensions for each node in a cluster and then including them in a matrix where the number of its rows refers to the total number of cluster members. Thereafter, a normalized version of this matrix is considered to be then multiplied by the local-weight vector, found in step 2, which ultimately results in obtaining the global weight vector. Interestingly, in our proposed protocol, the control message, sent by the fog node, has a massive information in which the nodes of each cluster are ordered in a list in a descending order based on their global weights. Actually, the top two nodes will serve as a CH and LH, respectively, for that cluster in the current batch (i.e., group of rounds) while the next top two nodes will serve as a CH and LH, respectively, for that cluster in the next batch and so forth. The batch duration is determined by the fog node which is assumed to be in a knowledge of all messages' exchanges between all nodes in the network along with their costs. In addition to aforementioned control message information, the round numbers at which the nodes alternate their heads are included. The criterion of alternating among batches is as follows. Both heads selected will stay serving in their roles as long as their energy consumption, until the current round, equals or does not exceed an energy threshold, E_{Thrs}. This criterion helps in maintaining a balance in the energy consumption among cluster's nodes. Literally, the global-weight list is subject to change as soon as any of the heads ran out of energy. In other words, the informative control message, sent by the fog node, includes further the new global-weight lists that should be considered by all clusters' members along their activation rounds. The main reason of making the whole task to be handled by the fog node is to reduce the control overhead which will be required, from sensor nodes, for achieving this purpose.

3.6. Genetic relay node selection algorithm

The genetic algorithm is an adaptive heuristic search algorithm that mimics the genetic concepts of natural selection, mating, mutation, and inheritance and is widely utilized in optimizing plenty of research problems [43]. The genetic algorithm starts with a set of randomly generated probable solutions, known as the initial population. Each individual is represented through an array or a string of genes called a chromosome, where the length of all chromosomes in the population should be equal. Every permissible gene should be evaluated via a fitness function to estimate its efficiency. Hence, the fitness function has to be formulated in

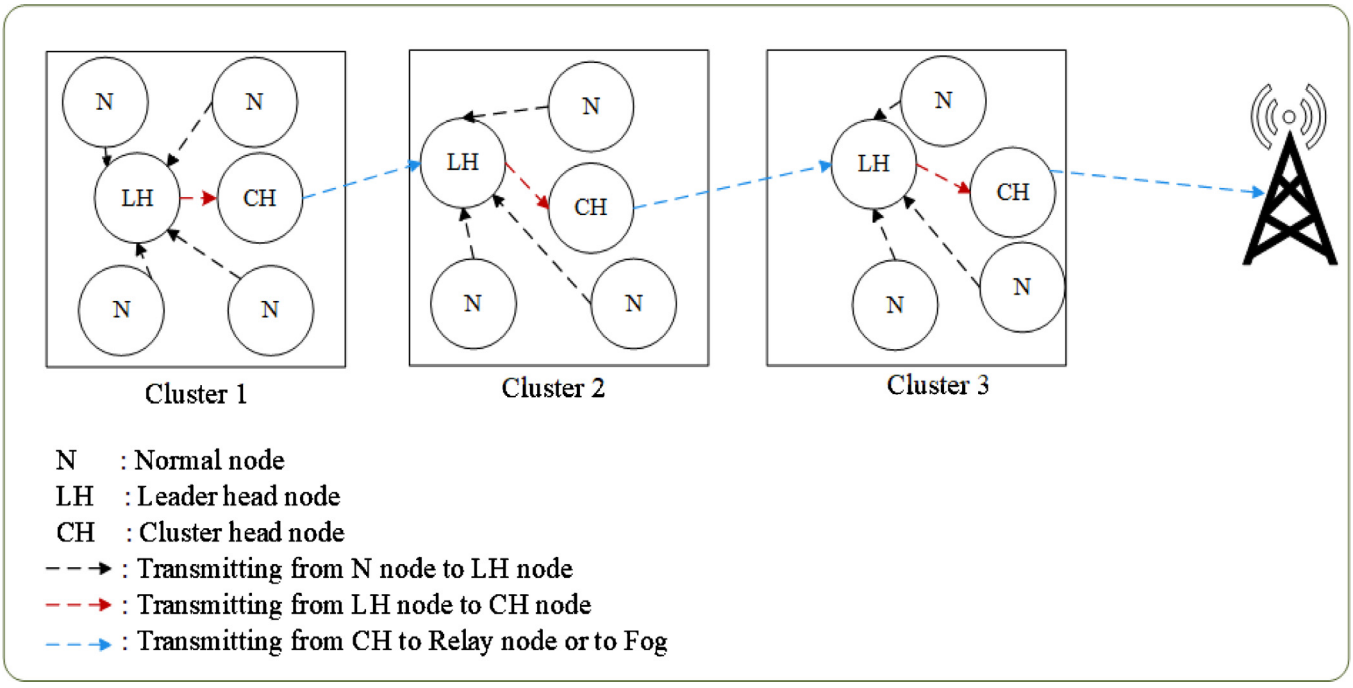

Fig. 6. The procedure of forwarding the sensed data of IoT environment toward the fog node.

such a way that a permissible gene provides a result around the optimum solution.

In the context of IoT sensors and for any cluster, if the distance between the CH and fog node exceeds the threshold distance, then the employment of relay nodes will become feasible, as shown in Fig. 6. Therefore, all LHs or CLs in the network are considered initially as candidate relay nodes. Upon satisfying a criterion, those filtered heads will turn out to be permissible relay nodes. This criterion involves three conditions where the first condition relates to that, for any cluster, the distance from the corresponding CH to a candidate relay node should not transcend the threshold distance. This can be justified due to making sure that there is no need to consider any further relay in between. The second condition refers to that the distance from a candidate relay node to the fog node should be less than the distance from the CH to the fog node. This condition is chosen to insure that the candidate relay node should be in the direction toward the fog node. The last one relates to that the energy of the candidate relay node should be greater than or equal to the average energy of all candidate relay nodes. As mentioned when discussing the AHP heads selection model, the fog node is in charge of finding the relay node for every CH or CL in any round, as shown in Fig. 4. In other words, the control message, sent by the fog node, will keep all CHs or CLs informed of their optimal relay nodes in every round. That is why the energy concern is included in the aforementioned criterion. However, for any cluster, there might be a number of possible hops for forwarding its traffic toward the fog node (RE_{num}), which can be expressed as

$$RE_{num} = ceil\left(\frac{\left(\left(y_{fog}-y_{CH}\right)^2+\left(x_{fog}-x_{CH}\right)^2\right)^{0.5}}{d_{Thres}}\right). \tag{14}$$

After finding the permissible relay nodes for all clusters in the network, the initial population can be determined, which consists mainly of many chromosomes. Indeed, each chromosome is made up of many genes where each gene belongs to one cluster and, in this context, refers to the permissible relay nodes. For instance, imagine there is a network in which four clusters are formed. This implies having 4 genes where each gene has a number of permissible relay nodes. As a follow-up to our prior example, the 4 genes, in sequence, have 2, 4, 3, and 5 permissible relay nodes, respectively. At this case, the initial population includes 5 chromosomes where the 5 permissible values, belong to the last gene, are spread out evenly among those chromosomes. In regards to the other three clusters, the permissible values are distributed alternatively among the 5 chromosomes. At this stage, finding the fitness value of each gene in each chromosome is initiated. The fitness function adopted in our algorithm (*FN*) is expressed as:

$$FN = \alpha \times f_1 + \beta \times f_2 + \gamma \times f_3, \tag{15}$$

where,f_1 represents the ratio of the energy of the current permissible relay node ($E_{res}(pe)$) to the average energy of all permissible relay nodes ($E_{avg-res}$). This reflects that the possibility of the current permissible relay node to be the optimal relay node gets high as its energy level is high. Moreover,f_2 denotes for the ratio of the average distances from all permissible relay nodes to the fog node, to the distance between the current permissible relay node and the fog node. As it gets closer to the fog node, the possibility of the current permissible relay node to be the optimal relay node increases. In addition, $f_3$refers to the ratio of the average number of times that all permissible relay nodes have become optimal relay nodes to the number of times the current permissible relay node played this role. In fact, this is an important concern. In different words, to achieve an efficient load balancing, if the current permissible relay node is already served in the prior rounds as the optimal relay node, then its possibility to serve longer will decrease. Lastly,α, β *and* $\gamma$are the fitness function coefficients which are experimentally chosen and listed in Table 2.

In light of the above discussion,$f_1$is expressed by

$$f_1 = \frac{E_{res}(pe)}{E_{avg-res}}, \tag{16}$$

Furthermore,$f_2$is given by

$$f_2 = \frac{\frac{\sum_{i=1}^{N}\left((y_{fog}-y_i)^2+(x_{fog}-x_i)^2\right)^{0.5}}{N}}{\left((y_{fog}-y_{pe})^2+(x_{fog}-x_{pe})^2\right)^{0.5}}. \tag{17}$$

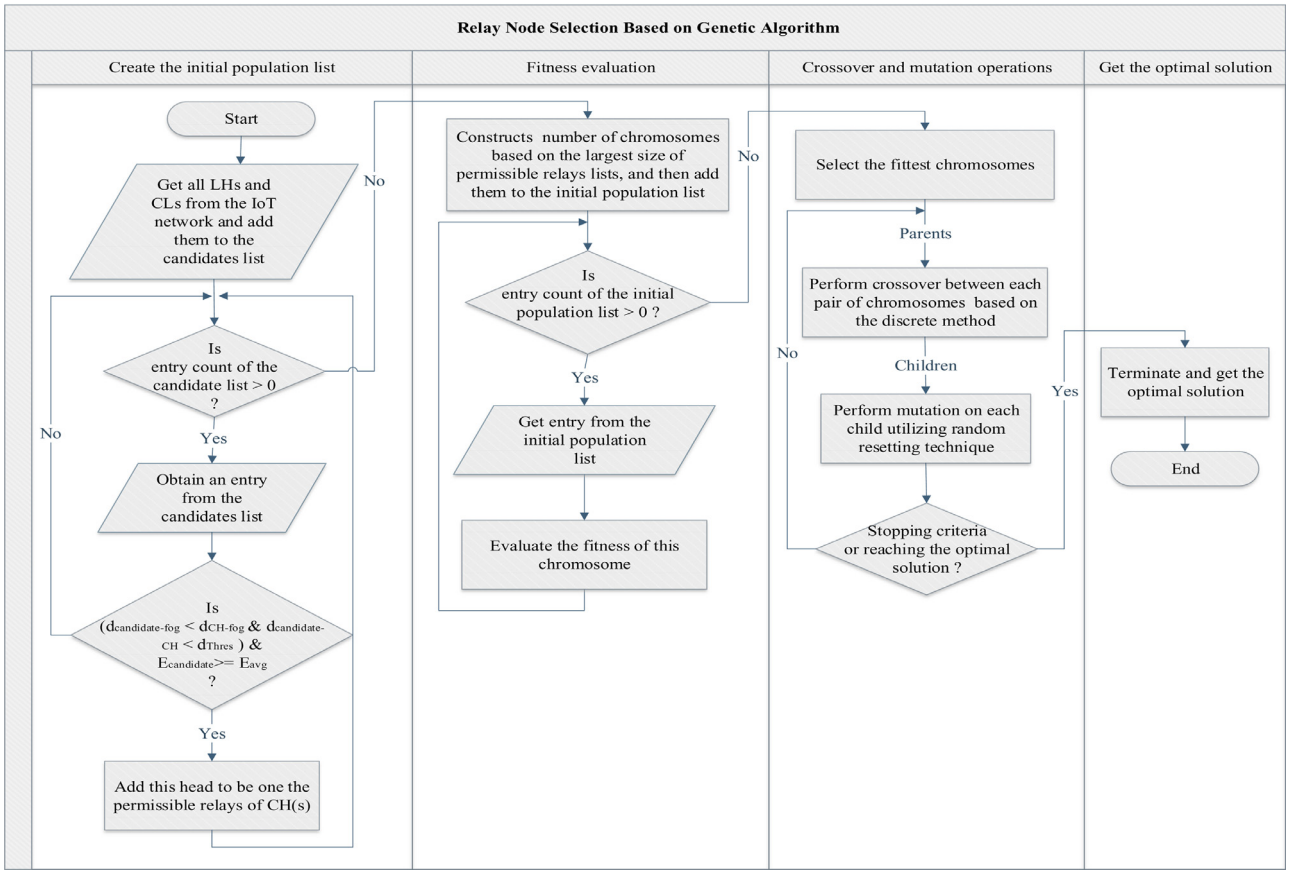

Fig. 7. Relay node selection using genetic algorithm.

At the end, f_3 is expressed by

$$f_3 = \frac{\sum_{i=1}^{N} C(i)}{\frac{N}{C(pe)}}, \tag{18}$$

where, $C(i)$ refers to the number of times that a permissible relay node i has become optimal relay node.

N refers to the population size (i.e., the number of permissible relay nodes).

At this point, the average of the fitness values of each chromosome is determined. If the average is beyond the boundaries (limits), then this chromosome will be excluded from the initial population. Genuinely, these limits are set based on the minimum and maximum acceptable values of the aforementioned fitness function. As soon as this task gets performed, the process of crossover is started taking into account that there are a lot of strategies available in the literature for this purpose out of which 1-point, k-point, shuffle, reduced surrogates, blend, uniform, heuristic uniform, and discrete crossover where the latter is employed in this work [43], which results in having new children. At this instance, those children will be the new population. After conducting a crossover process, there is a possible mutation outcome where there are many mutations approaches currently available such as bit flip, swap, scramble, and random resetting mutation, which is adopted in this research [44]. Attractively, after a mutation process, there might be a new gene which did not exist among the parents' genes, which is quite realistic. The process of conducting crossover operations and then mutations will be repeated in all generated children till to get one child (chromosome) which represents the optimal solution, where the whole procedure is demonstrated in Fig. 7. In other words, it represents the optimal relay node for every CH or CL. A complete example to show the entire technique is provided in Appendix B.

3.7. Avoiding intra- and inter-cluster interferences algorithm

The rapid proliferation of IoT technology leads to the emergence of a massive number of wireless communication technologies, such as RFID, Telensa, SigFox, LoRaWAN and NB-IoT that could share the same frequency bands in numerous scenarios. Based on this, many signals will be carried through the same frequency band which may lead to the data loss, higher delays, intermittent network connections, and lower network throughput due to signals' interferences that are caused by intra- and inter-cluster communication [45]. To eliminate these interferences, we utilize sensors which are embedded with multi-band antennas in both transmitting and receiving circuits, thereby enabling the use of different communication protocols. These protocols support the Frequency-hopping Spread Spectrum (FHSS) technique in order to enable the fog node to oblige all the sensors in the network area to utilize different frequencies and hence evade any possibility of communication jamming. To achieve these objectives, we employ the mechanism which is explained below and shown in Fig. 8.

a) The inter-cluster interferences, that could happen at the end of each round, is evaded by compelling each CH or CL to transmit over different frequencies considering the following cases:
   - In the case of having homogeneous or heterogeneous CHs or LHs operating over the same or various communication protocols with different frequencies, then there will be no possibility for any interference.
   - If the CHs support different or identical communication protocols that operate over the same range of frequencies, then the fog node will apply FHSS technique to let these heads transmit over distinctive frequencies.

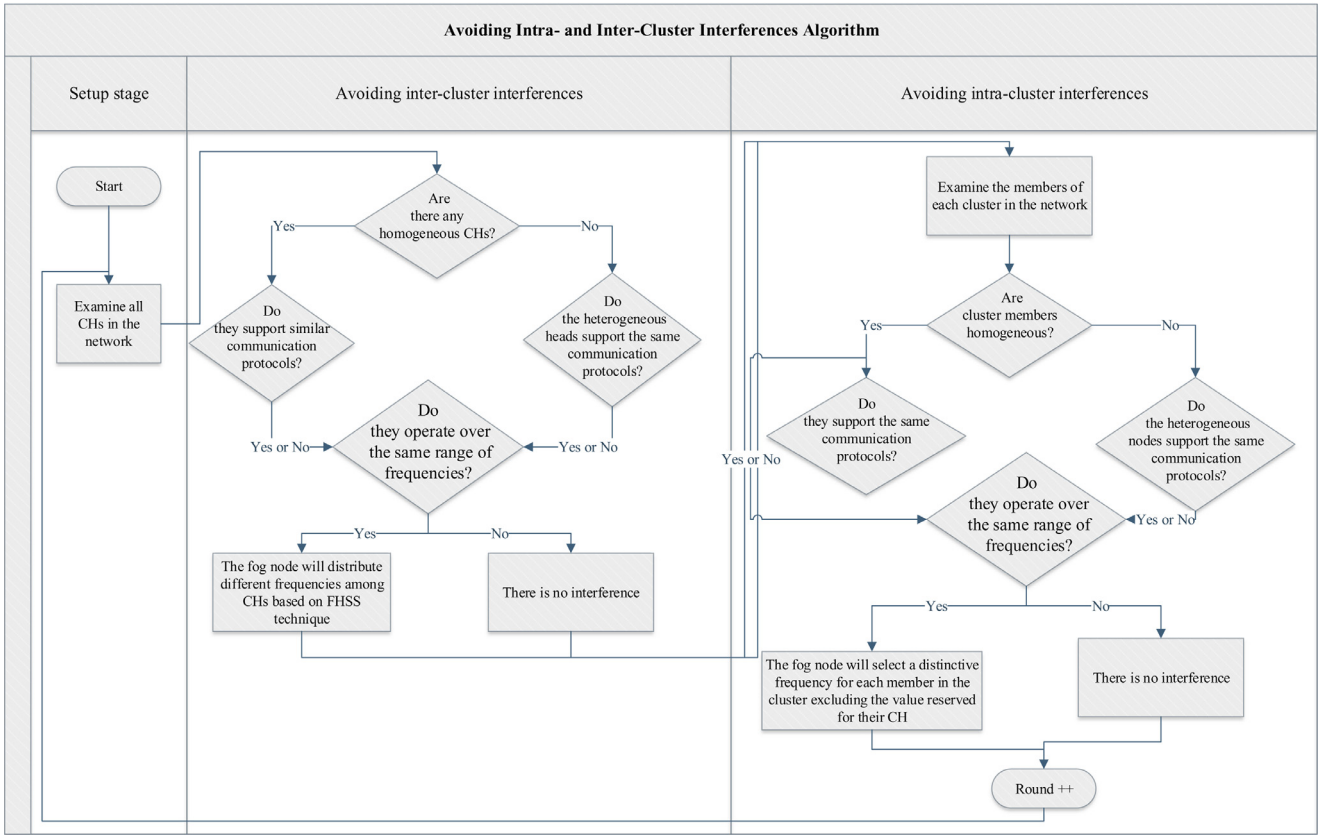

Fig. 8. Evading the interferences of intra- and inter-cluster communications in IoT network.

b) The signals' interferences, which may be caused by the intra-cluster communications among the members of a cluster, is possible to be avoided. In particular, after assigning specific frequencies to all CHs in the network area, as mentioned in the first step, the fog node will assign frequencies to cluster members bearing in mind the following cases:
   - If the members of a cluster have different or the same communication protocols and operate over the same range of frequencies, then the fog node will force them to transmit over distinctive frequencies excluding the frequency that is reserved for their CH.
   - If the cluster's sensors operate over distinctive or similar communication protocols that support different frequencies, then there will be no interference.

c) Due to obeying a batch-based style, the fog node switches the CH role among CHs in the network irregularly. In other words, not all the CHs will serve the same number of rounds (i.e., the batch length is different). Therefore, in our algorithm, the fog node, when preparing the setup parameters, is aware of all frequencies assigned to all nodes in the network in every round, hereby avoiding any interference that may arise by intra- or inter-cluster communications. However, Fig. 9 summarizes all algorithms considered in our proposed protocol.

4. Simulation results and discussion

In this section, a massive number of simulations has been conducted for evaluating and analyzing the performance of our proposed protocol. In other words, we firstly introduce the simulation environment and parameters used. Secondly, we define the performance metrics that are used in showing to what extent the contributions of our proposed protocol are significant. Finally, the simulation results along with necessary decisions are provided.

4.1. Simulation environment

The interest in enhancing different factors and parameters that affect the performance of IoT environments by the researcher's community is rapidly increasing. Accordingly, numerous experimental and simulation platforms have been developed due to being almost impossible to proceed in a real environment where many burdens, that face the setup and implementation in such environments like complexity, time, and cost, may exist. We were eager to choose an environment that can be equipped with different smart services for the reason of considering different scenarios of smart city applications. Consequently, we choose an informative geographical territory, which is Birdsboro borough, where different smart sensing technologies can be deployed and managed easily, hence, improving the life quality of citizens and tourists. Actually, different IoT applications may be considered in this simulated region such as smart traffic management, smart structural health of buildings, smart air quality management, smart parking, smart street lighting, etc. In this research, we use four focal software applications, where various types of sensors are deployed based on specific distributions that refer to the sensor type and its transmission range, which include Google Earth Pro v7.3.2.5776, OpenStreetMap web application, Autodesk AutoCAD vM.107.0, as well as MATLAB R2015a v8.5.0.197613. In our simulation experiments, 100 IoT nodes are deployed using various distributions, as summarized in Table 1, over an area of the size 60 m $\times$ 120 m. Furthermore, the simulation parameters used are provided in Table 2 and mainly considered as the default values unless otherwise mentioned in the discussion. The procedure used to acquire the essential information to conduct the simulations, such as buildings, parking lots and street coordinates is illustrated as:

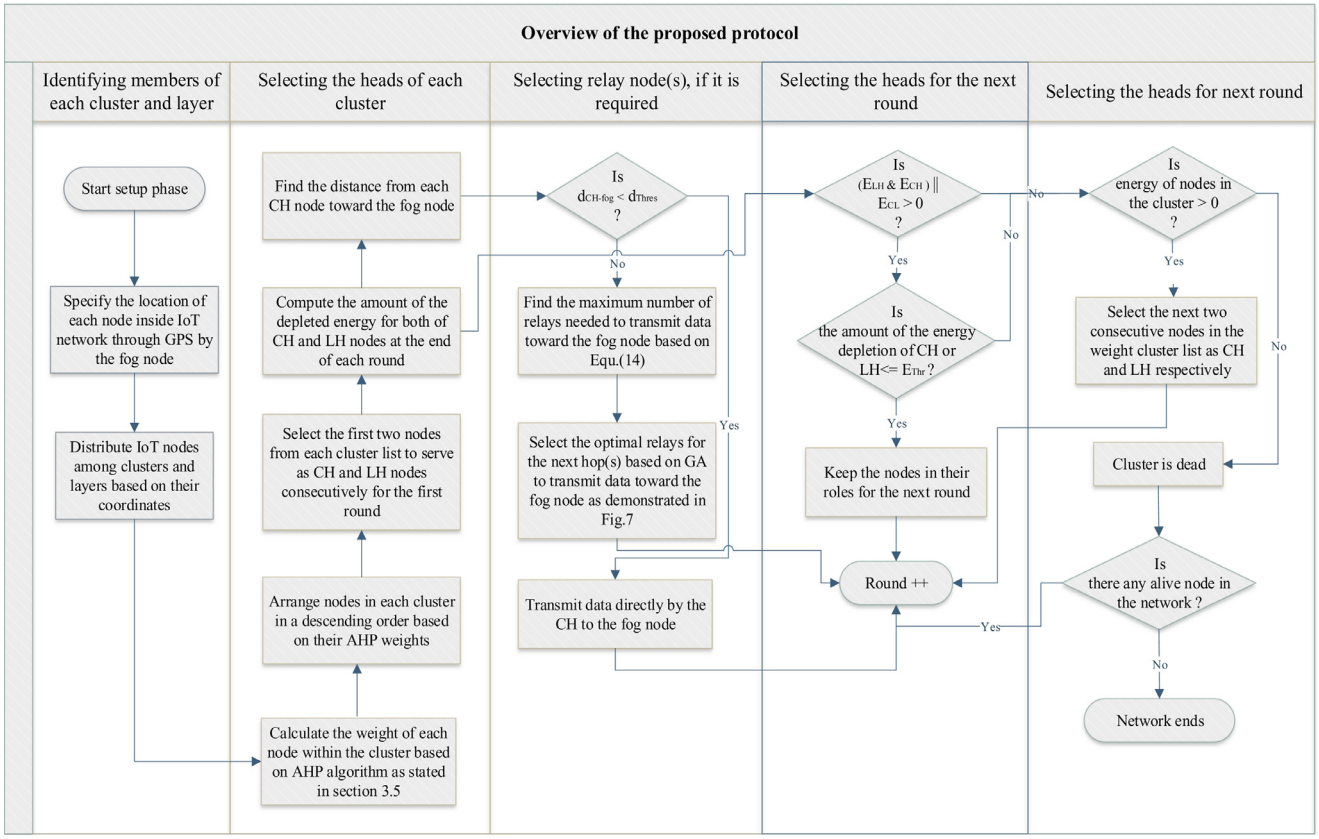

Fig. 9. Overview of the LiM-AHP-G-C protocola).

Table 1
IoT sensors and distributions in various network sizes.

IoT sensors		Distribution	Communication Protocol(s)	Number of sensors for (60 m × 120 m)	Number of sensors for (80m × 160m)	Number of sensors for (100 m × 200 m)	Number of sensors for (160 m × 320 m)
1	Smart parking sensors	Uniform distribution	RFID	25	45	70	190
2	Street light sensors	Uniform distribution [46]	Telensa	8	11	14	22
3	Smart traffic light	Roads Intersections	NB-IoT	8	8	8	8
4	Traffic congestion sensors	Random deployment [47]	Telensa LoRaWAN	6	18	31	80
5	Air quality sensors	Gaussian distribution [48]	Telensa	15	27	44	120
6	Waste management sensors (smart bins)	Random distribution	Telensa	20	36	58	155
7	Structural building	Particle swarm optimization algorithm [49]	SigFox	18	33	53	136
Total number of sensors				**100**	**178**	**278**	**711**

a) The designated area is specified and selected via Google Earth Pro App, where Birdsboro borough is chosen to be the region of interest, as shown in Fig. 10.
b) An OSM file is exported to identify the coordinates of all streets and buildings of Birdsboro borough using OpenStreetMap, as depicted in Fig. 11.
c) The OSM file is then imported into AutoCAD App after being converted into KMZ format.
d) The coordinates of traffic lights, structural health building, parking sensors, and all streets, as shown in Fig. 12, which are disseminated based on specific distributions, are then exported from AutoCAD into XLS files.
e) After importing all XLS files, generated from AutoCAD, into MATLAB, the coordinates of all aforementioned sensors are now known and accordingly, the simulation process begins as soon as the step below is considered.

Table 2
Simulation parameters.

Parameter	Value
Network size	60 m × 120 m
Cluster dimensions (height and width)	15 m × 30 m
Eq. (4) coefficients	δ=4, σ =8
E_{Thrs}	1mJ
Fitness function coeffitients	α = 0.5, β= 0.4, γ= 0.1
Fog node location	X=30, Y= −60
Number of IoT nodes	100 nodes
Data message size	6400 bits
Control message Size	200 bits
The initial energy of a node	0.5J
$\epsilon_{free-space-amp}$	10 PJ / bit / m^2
$\epsilon_{two-ray-amp}$	0.0013 pJ/bit/ m^4
E_{elec}	50 nJ/bit
E_{DA}	5 nJ/bit
$d_{crossover}$	100 m

Communication protocol name	**RFID [50] [51]**	**Telensa [52]**	**NB-IoT [53]**	**LoRaWAN [54]**	**SigFox [53]**
Communication protocol frequencies	(125–134) kHz 13.56 MHz (60–865) MHz (902–928) MHz	60MHz 200MHz 433MHz 470MHz 868Mhz 915MHz	850–900 Hz 3.75 kHz 15 kHz 180–200 kHz	100Hz 869MHz 915 MHz	200 kHz (868–869) MHz (902–928) MHz
Communication protocol transmission ranges	(1–10) cm (1–30) m	3km 20km	1 km 10 km	(2–5) km 15km	(3–10) km (30–50) km

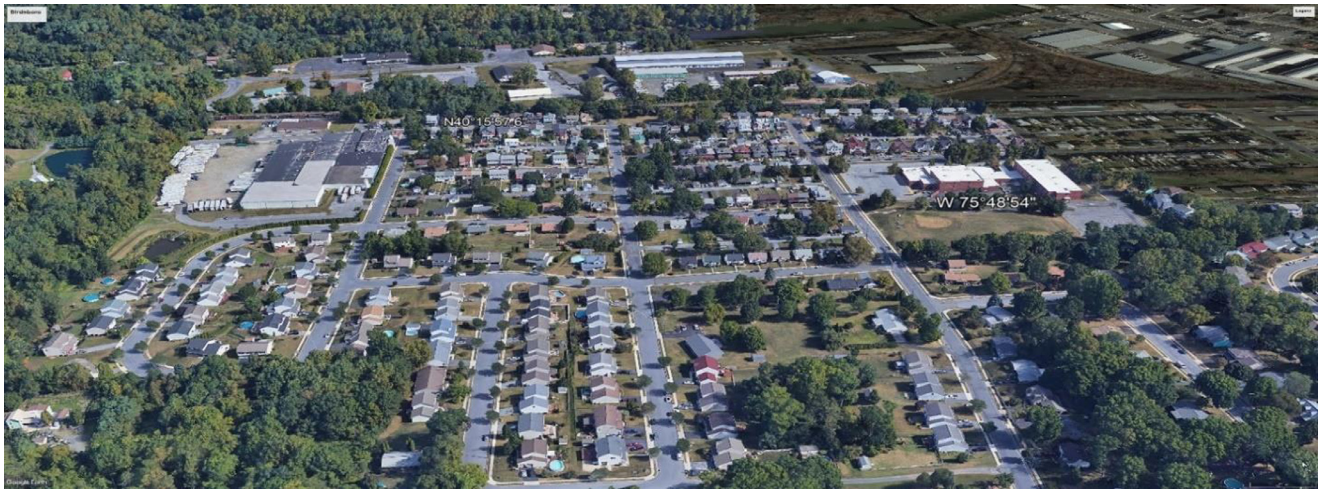

Fig. 10. Google earth map of Birdsboro borough in Pennsylvania, United States.

f) The locations of the other sensors, which are of interest too and include the street lights, traffic congestion, air quality, and waste management, are determined directly through MATLAB based on their transmission ranges and appropriate distributions, where all considered sensors are detailed in Table 1.

4.2. Performance metrics

The efficiency and robustness of our proposed protocol have been examined thoroughly where a tremendous number of simulations were conducted considering the following performance metrics:

i. Network lifetime which has been assessed in three different perspectives, namely, the First-Node-to-Die (FND), Half-Node-to-Die (HND), as well as Last-Node-to-Die (LND) metrics. The FND denotes for the time gauged (in rounds) from the initial IoT network deployment until the first IoT sensor depletes its energy and subsequently dies. The LND represents the total time (in rounds) till all sensors exhaust completely their energy. Similarly, the HND refers to the number of rounds where exactly half of the sensors deplete their energy.

ii. Network utilization which primarily refers to the ratio of the energy consumed for data transmissions to the energy consumed for both data transmissions and control overhead.

4.3. Results and discussion

To validate the scope of correctness of our proposed protocol, many scenarios are considered. Firstly, we investigate the effect of enlarging the network size on the IoT network lifetime of LiM-AHP-G-C protocol and consequently declare the network size that maximizes the IoT network lifetime to be then considered in the subsequent scenarios. Secondly, we check into thoroughly the number of alive nodes versus the round number. It is worth mentioning that, from this scenario to the rest, we implement the directly connected protocols (i.e. COCA, UCR, EA-CRP) and accordingly incorporate their results to show how and to what extent our proposed protocol steps the literature. Thirdly, we examine the FND against different network sizes. Fourthly, the LND is investigated under the consideration of having various network sizes. Fifthly, we explore the impact of employing different network sizes on the net-

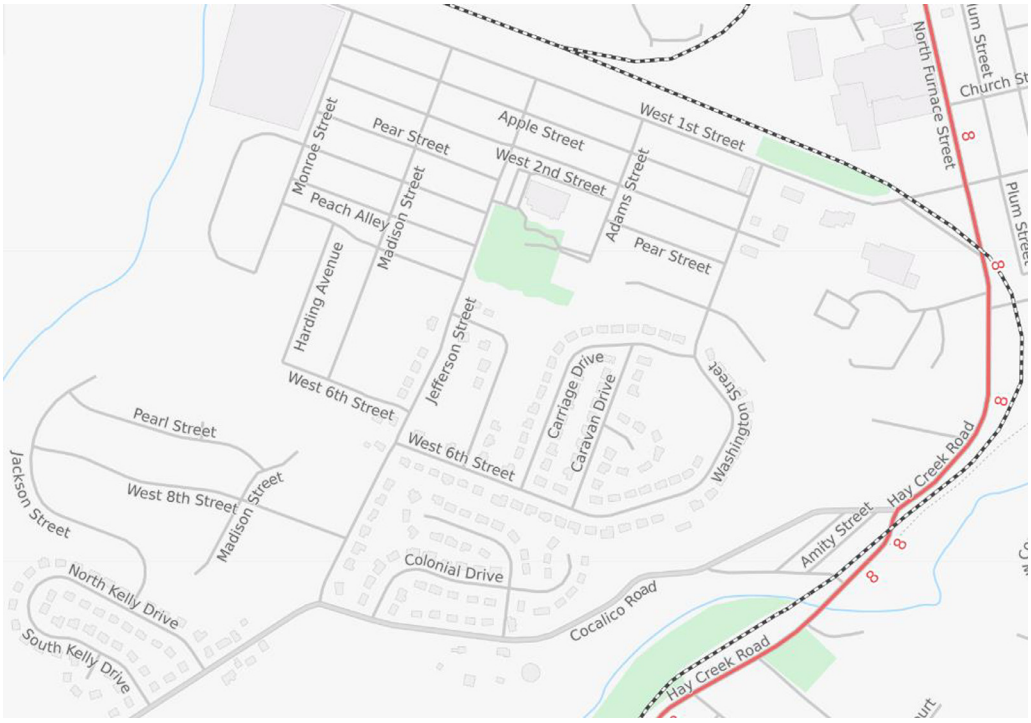

Fig. 11. Birdsboro borough buildings and streets by OpenStreetMap.

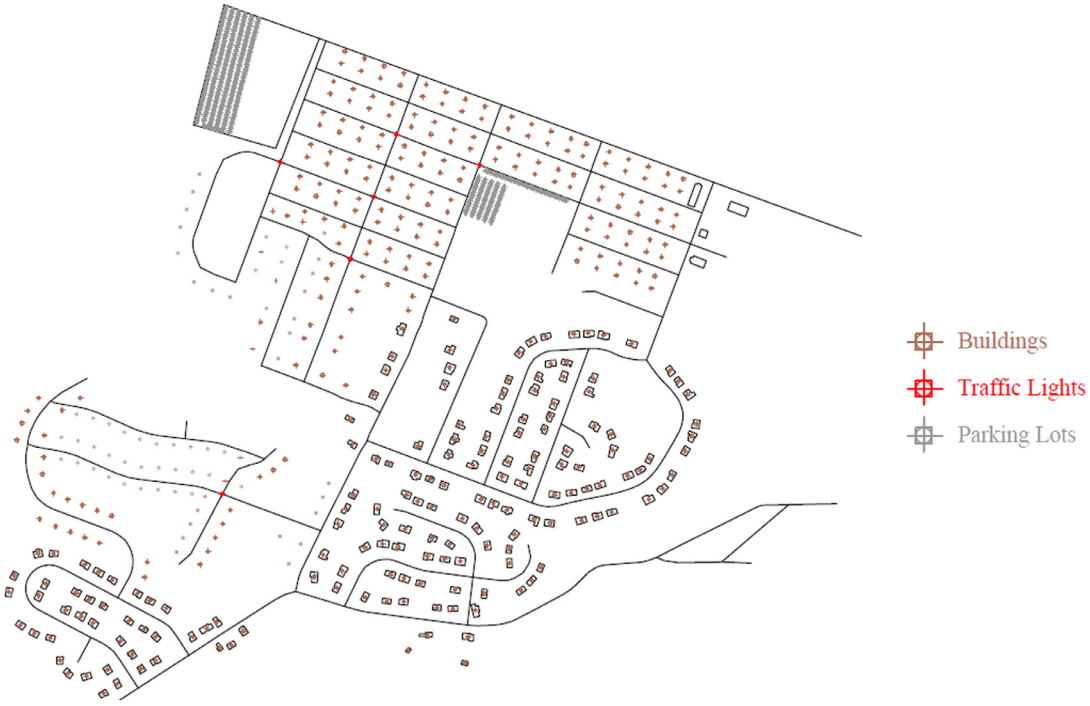

Fig. 12. Distribution of different types of IoT sensors through AutoCAD.

work utilization considering all aforementioned protocols. Finally, we examine the effect of increasing the initial energy of the IoT smart devices on the network lifetime of our protocol and other related protocols.

4.3.1. Simulation scenario1: define the suitable network size

In this scenario, we inspect how increasing the network size affects the IoT network time of our proposed protocol. Therefore, various network sizes are considered, which include (60 m × 120 m), (80 m × 160 m), (100 m × 200 m) and (160 m × 320 m). To keep the density of all aforementioned areas matches the network density, which is equal to 0.014 node/m^2, the number of sensors considered, in these areas, are 100, 178, 278, and 711 IoT sensors, respectively, which are classified based on their types, as shown in Table 1. Referring to Section 3.3 (division of network area algorithm), these areas are partitioned into 2, 3, 4 and 6 layers, as indicated in Table 3.

From Fig. 13, it can be clearly observed that the IoT network lifespan gets worse when the IoT network size increases which is to be expected since as the size of the IoT network increases more and more,

Table 3
The number of layers and clusters in various network areas.

Number of layers VS number of clusters	(60 m x 120)		(80 m x 160 m)			(100 m x 200 m)				(160 m x 320 m)					
Number of layers	2		3			4				6					
Number of clusters in each layer	4	12	4	12	20	4	12	20	28	4	12	20	28	36	44
Total number of clusters in the network	**16**		**36**			**64**				**144**					

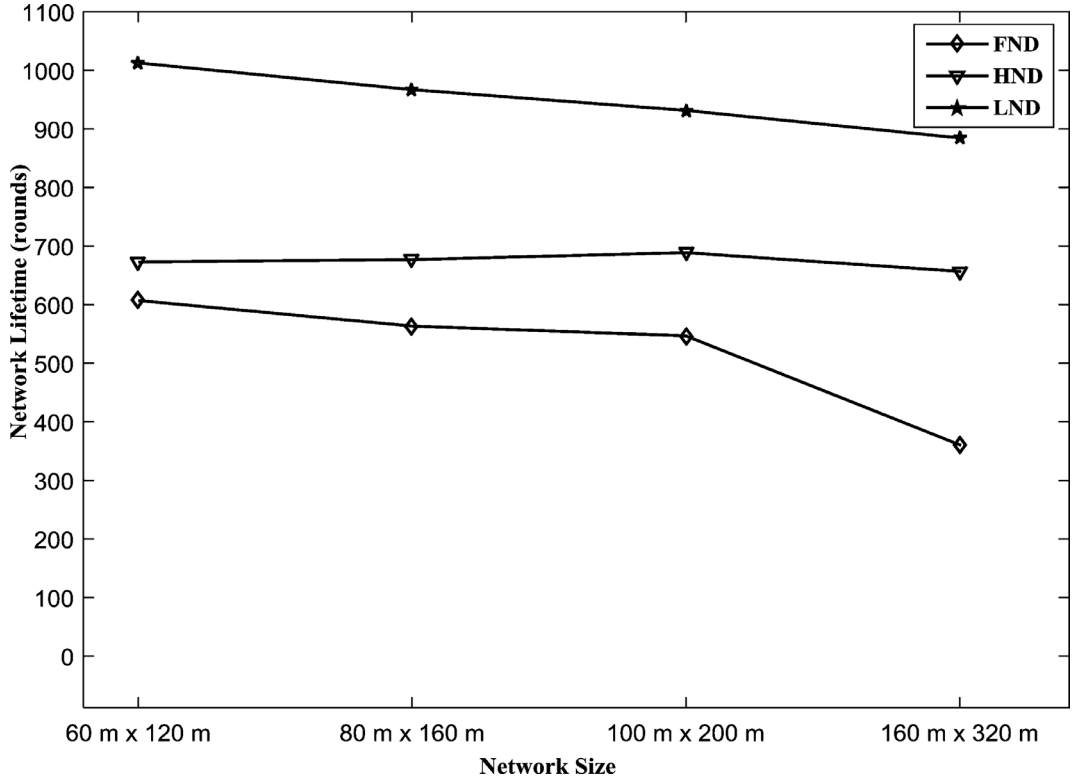

Fig. 13. Network lifetime of LiM-AHP-G-C protocol versus different IoT network sizes.

the communication distances between nodes and their heads and further between heads and the fog node get longer and longer, causing a rapid network energy depletion. As it shows the best IoT network lifetime, we choose the area, (60 m × 120 m), as a default network size in the subsequent scenarios.

4.3.2. Simulation scenario 2: number of alive nodes versus round number

In this scenario and as shown in Fig. 14, the number of alive IoT sensors is described in every round considering the LiM-AHP-G-C protocol and its counterparts. An overarching common trend can be noticed from this figure, that is, the number of alive nodes decreases as the number of rounds increases in all protocols which is to be expected as the number of rounds increases more and more, the amount of messages' exchanges increases more and more which gives rise to getting closer to the network termination. Interestingly, we can clearly notice, from this figure, that the proposed protocol surpasses all the other protocols in terms of the number of alive nodes per round in which the network stays functioning for 1013 rounds while the networks in the other protocols, namely, COCA, UCR, and EA-CRP, remain alive for 231, 351 and 577 rounds, respectively, which result in having improvements of 338.5 %, 188.6% and 75.6% over COCA, UCR, and EA-CRP protocols, respectively. This superb enhancement is attributed to the contributions of the following ideas that are incorporated into LiM-AHP-G-C protocol. Firstly, the procedure of partitioning the network area into a multi-layered architecture in which each layer differs among the others in the number of equal-sized clusters wherein, as seen in Fig. 2, has absolutely a favorable influence on preserving the overall IoT network energy as most of messages' exchanges are kept under the use of Friis free space channel propagation model. Secondly, dissimilar to what is used in the directly connected protocols, the setup overhead is entirely excluded in all rounds but round one where the task is handled by the fog node which results in reducing the control overhead and consequently prolonging the IoT network lifetime. Thirdly, the employment of AHP algorithm for choosing the CHs and LHs (or CLs) along with rotating the heads' roles among cluster members based on a batch-based time-division approach lead to distributing the energy consumption evenly among sensor nodes. Finally, the usage of genetic algorithm for selecting relay nodes to forward the aggregated data from CHs, which are distant more than the threshold distance away from the fog node, maintains the undergo of Friis free space channel propagation model.

The EA-CRP performs better than COCA and UCR protocols which is attributed to employing a multilayered structure, where the sizes of layers decrease toward the fog node. As a consequence, the EA-CRP minifies the long-distance communications, required for intra-cluster communications, and therefore, preserves the energy of those nodes, located closer to the fog node, for the inter-cluster communications instead, thereby achieving some kind of a balance in the energy consumption. Furthermore, in the EA-CRP, two heads are used (i.e., CH and LH) for the reason of distributing the energy consumption among them when receiving, aggregating and transmitting cluster messages. Additionally, a multi-hop routing technique is operated in which both the node residual energy and its distance toward the fog node are involved when choosing the relay node, thereby mitigating the energy required for communicating with the fog node.

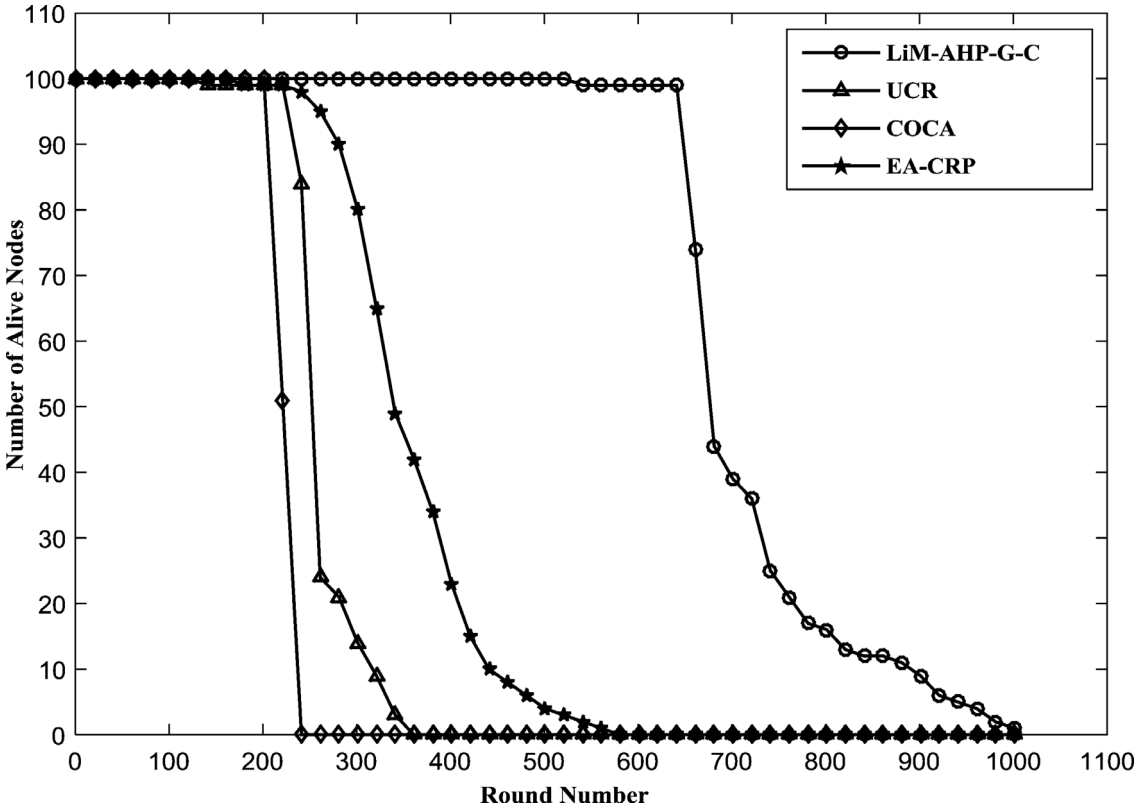

Fig. 14. Number of alive sensors against round number considering different protocols.

On the other hand, in the COCA protocol, the network area is partitioned into square units of equal sizes by dividing the length of the network over its width (i.e., having just two units over the network area chosen). In addition, the number of clusters in each unit increases as of getting closer to the fog node. In the COCA protocol, the impact of utilizing long-distance communications is totally neglected while addressing the power consumption problem. Above all, the CHs in the COCA protocol choose the relaying node randomly. In other words, there is a possible case where the relay nodes selected will almost run out of energy, causing data loss and shorter IoT network lifetime. Also, in the COCA protocol, the clusters are reconstructed in every round, hereby increasing the control overhead. The aforementioned reasons make the COCA protocol exhibit remarkably the worst behavior among the other protocols. Notably, the UCR protocol acts better than the COCA protocol. Actually, in the UCR protocol, the broadcast range used does not change with round. The CHs are further chosen arbitrary. In other words, sensors with low energy are eligible to be CHs. Moreover, the network is flooded with a tremendous number of control messages every round such as *COMPETE_HEAD-MSG, FINAL_HEAD_MSG*, and *QUIT_ELECTION_MSG*, letting the nodes to exhausted their energy so early. It is good to stress on the point that the relay nodes are selected in a way that the CH may need to communicate directly with the fog node as long as its energy exceeds that in the relay node, causing a rapid node's death.

4.3.3. Simulation scenario 3: FND against network size

Fig. 15 depicts the FND against the network sizes of (60 m × 120 m), (80 m ×160 m), (100 m × 200 m), and (160 m × 320 m) considering the LiM-AHP-G-C protocol and its counterparts. Although it occurs too early in the other protocols, the FND, in the LiM-AHP-G-C protocol, makes the network function at least three times what is achieved in the other protocols. In specific, the FND achieved in the LiM-AHP-G-C protocol is at round 607 while in the other protocols, namely, COCA, UCR, and EA-CRP, its values are at 210, 223 and 218 rounds, respectively considering, of course, the network size 60 m × 120 m. This is owing to the energy-aware algorithms that are employed in our protocol, which are illustrated and highlighted extensively in the previous scenarios.

4.3.4. Simulation scenario 4: LND in opposition to network size

This scenario examines the LND in opposition to the network size considering LiM-AHP-G-C, COCA, UCR, and EA-CRP protocols where its results are plotted in Fig. 16. The network sizes considered are the same as those discussed in the prior scenarios. The contributions of the LiM-AHP-G-C protocol are significant and undeniable. In particular, the LND, for the network size of 60 m × 120 m, is at 1013 rounds while in COCA, UCR, and EA-CRP protocols, it is at 231, 351 and 577 rounds, respectively. Similarly, for the network size of 160 m ×320 m, the FND is at 607, 210, 223, and 218 rounds for the LiM-AHP-G-C, COCA, UCR, and EA-CRP protocols, respectively.

4.3.5. Simulation scenario 5: network energy utilization against network size

To this end, it is of interest to know the impact of the control overhead encountered in our proposed on the overall network energy utilization. In other words, what is the quota of the energy consumed for the control overhead with respect to the overall energy consumption. To address this concern, Fig. 17 depicts the network utilization in contrast with the network size considering all aforementioned protocols. The network utilization(*NU*)is defined as the proportion of the energy consumed in data transmission (E_D) to the total IoT network energy (E_T), which is expressed as:

$$NU = \frac{E_D}{E_T}. \tag{19}$$

Among all protocols, our proposed protocol has the best network energy utilization. For instance and considering the network size of 60 m × 120 m, the network utilization in the LiM-AHP-G-C protocol approaches 98% while in the other protocols, that are, COCA, UCR, and

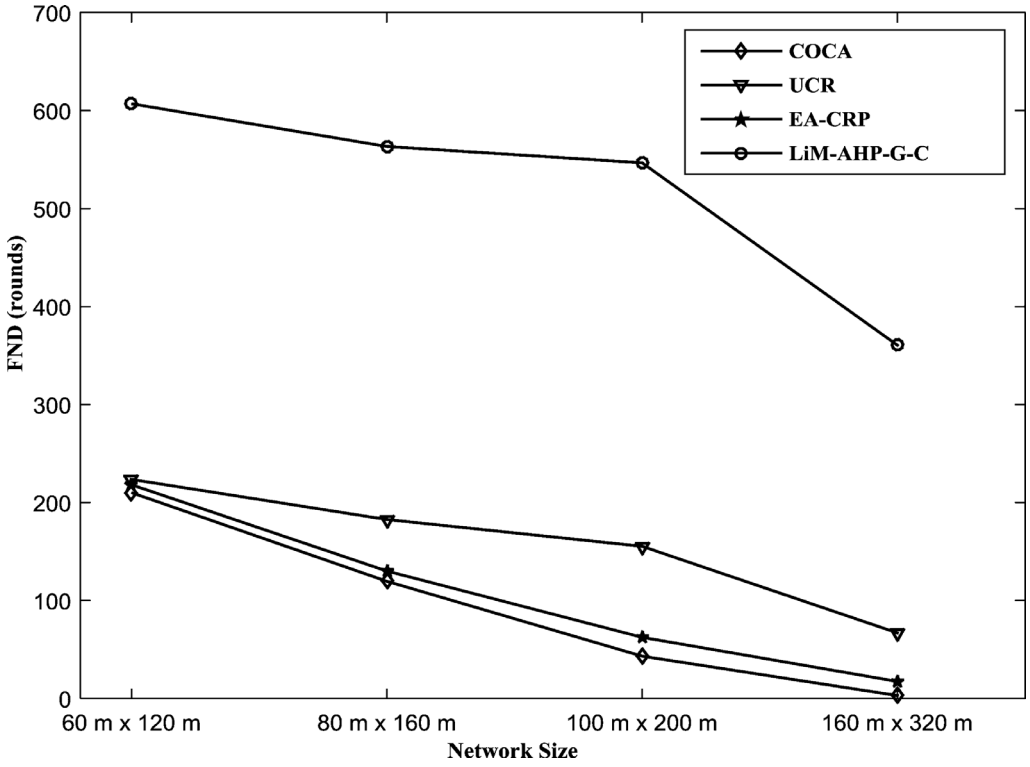

Fig. 15. FND against sensor field size considering different protocols.

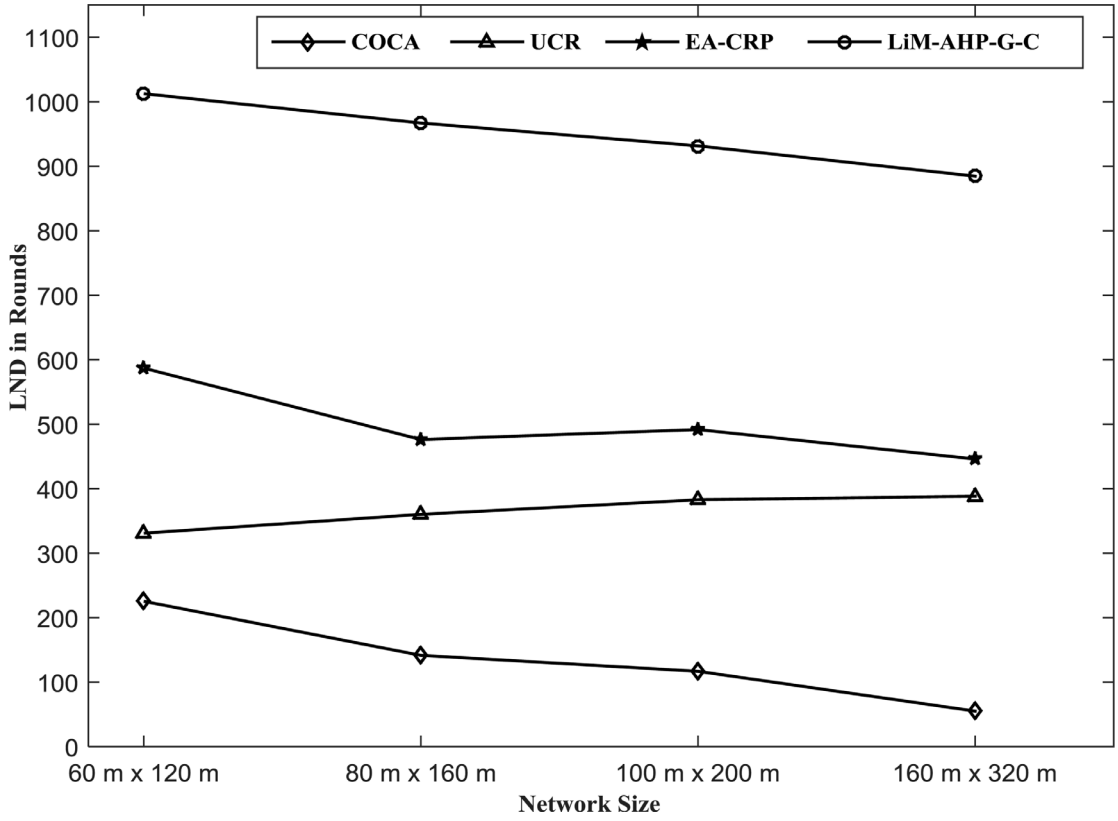

Fig. 16. LND in opposition to sensor field size considering various protocols.

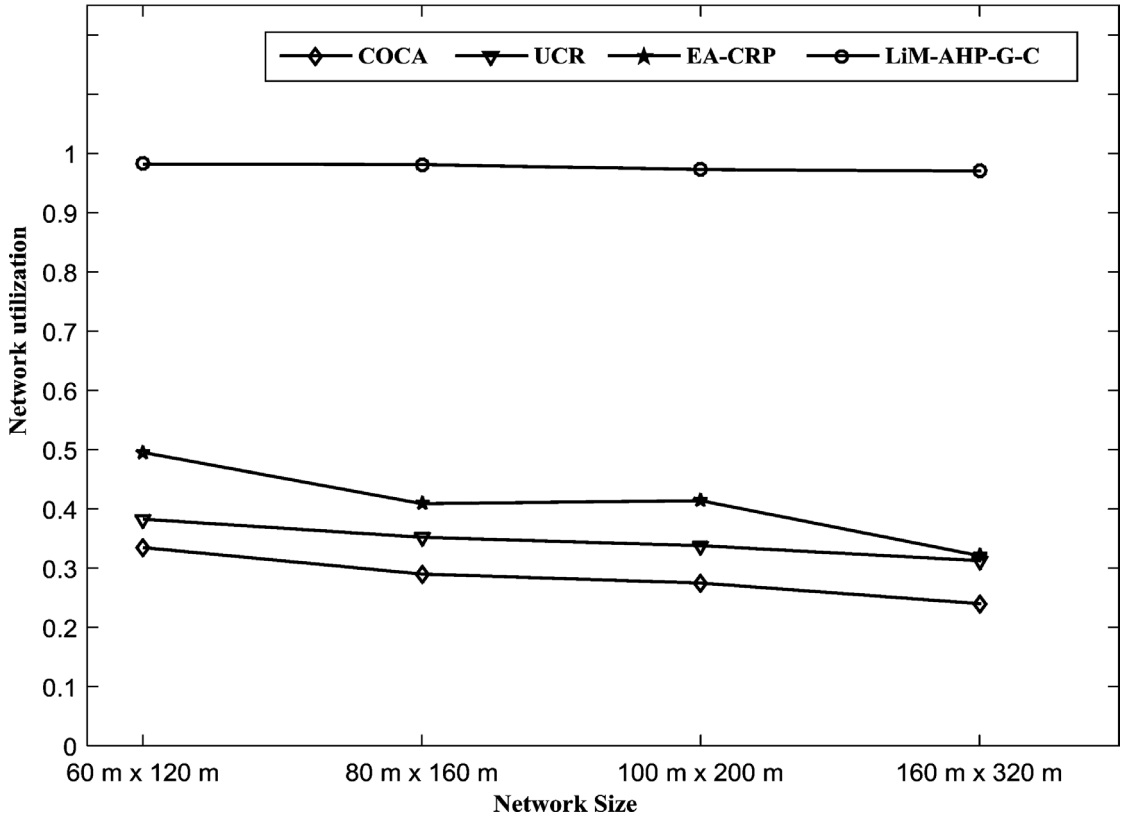

Fig. 17. Network energy utilization against sensor field size considering various protocols

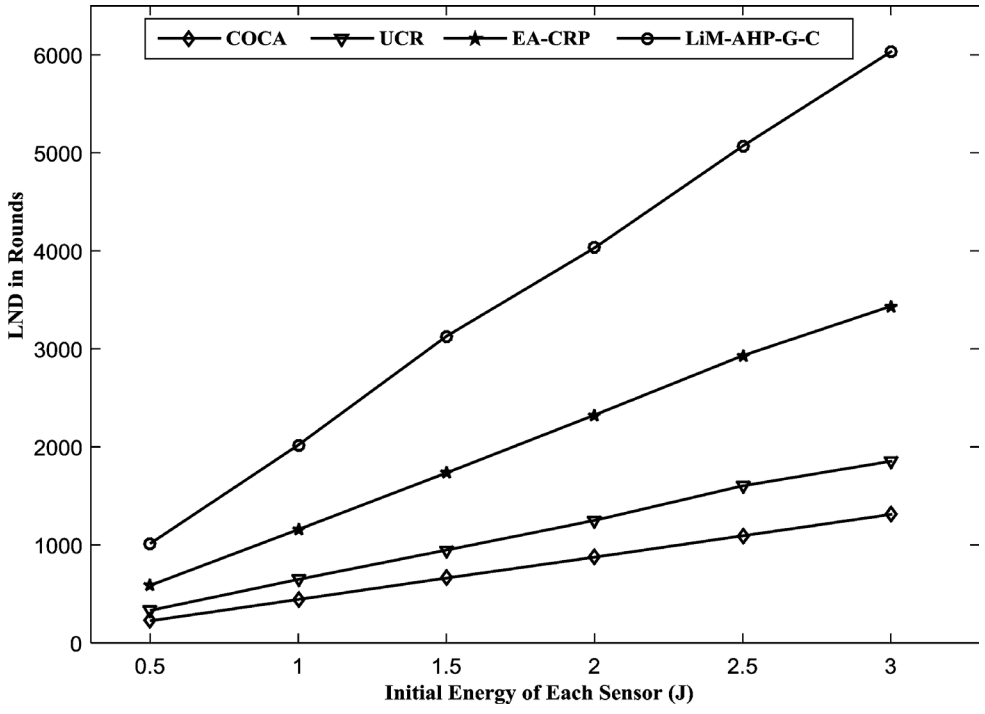

Fig. 18. LND opposite to initial energy considering various protocols.

EA-CRP, it approaches 33.5 %, 38.4%, and 49.5%, respectively. In a similar manner and considering the network size of 160 m × 320 m, it approaches 97%, 24%, 31.25% and 32.09% for LiM-AHP-G-C, COCA, UCR, and EA-CRP protocols, respectively. From these results, we can conclude that the control overhead in our proposed protocol is minimal. Furthermore, the scalability is achieved as the network utilization, in our proposed protocol, is much less sensitive to any change in the network size than others.

4.3.6. Simulation scenario 6: network lifetime opposite to initial energy

In this scenario and as shown in Fig. 18, the network lifespan, in terms of LND, opposite to the initial energy is examined considering our

proposed protocol and its counterparts, that are, COCA, UCR, and EA-CRP. The values of initial energy are 0.5, 1, 1.5, 2, 2.5, and 3J. It can be clearly noticed from this figure that the proposed protocol surpasses the other protocols for all initial energy values considered. In addition, as the initial energy increases, the performance of all protocols gets better which is to be expected as the increase in the initial energy reflects positively on the IoT network lifetime. Unlike its counterparts, the behavior of our proposed protocol has a superliner trend as the initial energy increases. In fact, the ideas or algorithms incorporated in our proposed protocol make it novel and extremely attractive.

5. Conclusions and future works

The IoT devices that are utilized in smart city applications are usually integrated with non-rechargeable and restricted batteries, making the IoT networks susceptible to a rapid energy depletion. Correspondingly, one of the most critical issues that have been drawing the attention of IoT researchers is how to conserve the energy of IoT network for the purpose of improving its lifetime and making it last for a long period. In this work, an energy-aware clustering and routing protocol, called LiM-AHP-G-C, is proposed which basically aims at mitigating the hindrances that may face the communication process of heterogeneous smart devices. The major findings of our proposed protocol can be briefed as follows. To begin with, it considers the configurations of a real IoT network where heterogeneous IoT sensors are deployed over Birdsboro borough. In addition, the network area chosen is divided into fixed-sized layers which further is split into equal-sized clusters. The number of layers and clusters in a layer are expressed experimentally in a way that the messages' exchanges are kept under the use of the Friis free space channel propagation model. On top of that, the heads are selected based on an AHP algorithm that is parameterized by node's residual energy, its distance to the fog node, and its average distance among cluster members. It does not end at this extent, but the heads' roles are rotated among cluster members based on a batch-based time-division approach which certainly account for making the nodes' deaths late as much as possible. Last but not least, an efficient genetic algorithm is employed to select potential nodes that are capable of relaying clusters' traffic to the fog node with addressing the major constraint of that the long-distance communications are to be kept minimum. It is worth mentioning that all of the above algorithms are performed once in a centralized and proactive fashion by the fog node. In other words, the rounds in LiM-AHP-G-C protocol are setup overhead free. The validity and effectiveness of our proposed protocol are exhibited via different simulated scenarios from the perspectives of IoT network lifetime and network energy utilization. In summary, the contributions of the LiM-AHP-G-C protocol are extremely magnificent where its performance significantly outperforms directly existing protocols (i.e., EA-CRP, COCA, UCR). As future directions to this work, adapting and examining multiple software define network controllers will be a valuable addition. Moreover, investigating the impact of energy heterogeneity of IoT sensors on the IoT network lifetime will be a good research issue. At the end, incorporating the mobility option will be a tremendous dilemma and a case study for many IoT researchers.

Declaration of Competing of Interest

None.

Appendix A

A.1. AHP model assumptions and values

In this appendix, all assumptions and values belong to our AHP model are detailed. In particular, the matrix$A$, which is discussed in (5) and represents pairwise comparisons between the three dimensions (i.e., the levels of importance among the dimensions) chosen, is assumed, when referring to Table A.1, as

$$A = \begin{pmatrix} 1 & 3 & 5 \\ 0.333 & 1 & 3 \\ 0.2 & 0.333 & 1 \end{pmatrix}. \tag{A.1}$$

Utilizing (8), the A_{norm} can be written as

$$A_{norm} = \begin{pmatrix} 0.6523 & 0.6923 & 0.5556 \\ 0.2174 & 0.2308 & 0.3333 \\ 0.1304 & 0.0769 & 0.1111 \end{pmatrix}. \tag{A.2}$$

Utilizing (A.2) on (7) yields the local-weight vector (6) as

$$w = \begin{pmatrix} 0.6334 \\ 0.2605 \\ 0.1061 \end{pmatrix}. \tag{A.3}$$

Multiplying (A.1) by (A.3) results in obtaining the weight sum vector,w_s, as

$$w_s = \begin{pmatrix} 1.9454 \\ 0.7897 \\ 0.3195 \end{pmatrix}. \tag{A.4}$$

Substituting (A.3) and (A.4) into (12), we obtain

$$CO = \begin{pmatrix} 3.0714 \\ 3.0315 \\ 3.0113 \end{pmatrix}. \tag{A.5}$$

Substituting (A.5) into (11) yields

$$\lambda = 3.0381. \tag{A.6}$$

Substituting (A.6) into (10) provides

$$CI = 0.01904. \tag{A.7}$$

Consequently, substituting (A.7) into (9) and getting the$RI$from Table A.2, we obtain

$$CR = \frac{0.01904}{0.58} = 0.0328. \tag{A.8}$$

Referring to the consistency check constraint, illustrated previously, the one just obtained is within the proposed range. Therefore, our assumptions concerning the levels of importance among dimensions chosen are valid.

To find how the global-weight vector is obtained, let us assume that there is a cluster that consists of eight nodes where their IDs, residual en-

Table A.1
A pairwise comparison scale [41].

Scale of a_{ij}	Interpretation
1	Equally important.
3	Moderately important.
5	Strongly more important.
7	Very Strongly more important.
9	Extremely important.

Table A.2
RI based on the number of dimensions [41].

Number of dimensions (m)	RI
2	0
3	0.58
4	0.9
5	1.12
6	1.24
7	1.32
8	1.41
9	1.45
10	1.51

Table A.3
Cluster members' energy and distances.

Node ID	Residual energy (J)	Distance to the fog node (m)	Average distance among cluster members (m)
3	0.65	2.895	2.0234
5	0.559	1.956	1.0525
15	0.7	0.658	3.0652
8	0.61	0.9881	3.2081
53	0.5	1.0351	1.7110
91	0.57	3.0037	2.8198
96	0.79	2.9750	3.0022
100	0.68	1.0058	2.5581

ergy, distance to the fog node, and average distance among other cluster members are all given in Table A.3.

With reference to the third step of Section 3.5 and the values of the three dimensions of all cluster members, which are shown in Table A.3, the normalized version of the generated matrix$B$(i.e., B_{norm}) can be obtained as

$$B_{norm} = normalization\ of \begin{pmatrix} 0.65 & 2.895 & 2.0234 \\ 0.559 & 1.965 & 1.0525 \\ 0.7 & 0.658 & 3.0652 \\ 0.61 & 0.9881 & 3.2081 \\ 0.5 & 1.0351 & 1.711 \\ 0.57 & 3.0037 & 2.8198 \\ 0.79 & 2.9750 & 3.0022 \\ 0.68 & 1.0058 & 2.5581 \end{pmatrix}$$

$$= \begin{pmatrix} 0.128484 & 0.199302 & 0.104083 \\ 0.110496 & 0.135277 & 0.05414 \\ 0.138367 & 0.045299 & 0.157672 \\ 0.120577 & 0.068024 & 0.165023 \\ 0.098834 & 0.07126 & 0.088013 \\ 0.11267 & 0.206785 & 0.145049 \\ 0.156157 & 0.204809 & 0.154432 \\ 0.134414 & 0.069243 & 0.131587 \end{pmatrix}. \quad (A.9)$$

Multiplying (A.9) by the local-weight vector, expressed in (A.3), results in having the following global-weight

$$W = \begin{pmatrix} 0.14434 \\ 0.11097 \\ 0.11617 \\ 0.11160 \\ 0.09050 \\ 0.14062 \\ 0.16864 \\ 0.11713 \end{pmatrix}. \quad (A.10)$$

It is noteworthy to mention that the control packet received from the fog node includes primarily all clusters' members sorted in descending orders with reference to their AHP global weights. Based on this and referring to the global-weight vector of a cluster consists of eight nodes, as shown in (A.10), Table A.4 shows the portion of the control packet belongs to this cluster. Consequently, each cluster member will be aware of the heads in each batch. For example, nodes 96 and 3 will serve as CH and LH, respectively, in the current batch, while nodes 91 and 100 will serve as CH and LH, respectively, for the next batch and so forth.

Appendix B

B.1. Selecting optimal relaying nodes

To comprehend the operation of the genetic algorithm adopted in this paper, let us assume that we have a number of CHs (i.e., CH1, CH4, CH6, CH11, CH25, CH29, CH31), which require to transmit their data via optimal relay nodes to the fog node. Referring to this discussion of our genetic algorithm, the following steps are considered:

1) Each gene in the chromosome represents a CH along with its permissible relay node, as shown in Fig. B.1.
2) Selects the fittest chromosomes from the initial population (i.e., selects the chromosomes where the averages of their genes' fitness values stick within the boundaries). Fig. B.2 shows the case where just four chromosomes are selected.
3) Conducts a crossover function, based on the discrete technique, between the fittest parents where, for example, the pattern of vector **V** [0 1 1 0 101] is chosen. Simply, the genes of the new children will be taken from the first and second parents if the val-

Table A.4
Control packet portion belongs to eight nodes cluster.

Node ID	3	5	15	8	53	91	96	100
Global weights	0.14434	0.11097	0.11617	0.11160	0.09050	0.14062	0.16864	0.11713
Node order	2	7	5	6	8	3	1	4

CH1	CH4	CH6	CH11	CH25	CH29	CH31
LH11	LH3	LH5	LH3	LH18	LH13	LH25

CH1	CH4	CH6	CH11	CH25	CH29	CH31
LH6	LH12	LH15	LH31	LH22	LH23	LH3

CH1	CH4	CH6	CH11	CH25	CH29	CH31
LH2	LH7	LH8	LH9	LH30	LH15	LH16

CH1	CH4	CH6	CH11	CH25	CH29	CH31
LH13	LH25	LH12	LH27	LH21	LH26	LH8

CH1	CH4	CH6	CH11	CH25	CH29	CH31
LH20	LH10	LH29	LH13	LH14	LH9	LH27

Fig. B.1. Initial population.

CH1	CH4	CH6	CH11	CH25	CH29	CH31
LH11	LH3	LH5	LH3	LH18	LH13	LH25

CH1	CH4	CH6	CH11	CH25	CH29	CH31
LH6	LH12	LH15	LH31	LH22	LH23	LH3

CH1	CH4	CH6	CH11	CH25	CH29	CH31
LH2	LH7	LH8	LH9	LH30	LH15	LH16

CH1	CH4	CH6	CH11	CH25	CH29	CH31
LH13	LH25	LH12	LH27	LH21	LH26	LH8

Fig. B.2. Fittest chromosomes.

CH1	CH4	CH6	CH11	CH25	CH29	CH31
LH11	LH7	LH8	LH3	LH30	LH13	LH16

CH1	CH4	CH6	CH11	CH25	CH29	CH31
LH6	LH25	LH12	LH31	LH21	LH23	LH8

Fig. B.3. New children after performing a crossover among parents.

CH1	CH4	CH6	CH11	CH25	CH29	CH31
LH11	LH7	LH8	LH8	LH30	LH13	LH16

CH1	CH4	CH6	CH11	CH25	CH29	CH31
LH6	LH25	LH12	LH25	LH21	LH23	LH8

Fig. B.4. New children after performing a mutation among children.

CH1	CH4	CH6	CH11	CH25	CH29	CH31
LH11	LH25	LH12	LH8	LH21	LH13	LH8

Fig. B.5. New child after conducting the second crossover.

CH1	CH4	CH6	CH11	CH25	CH29	CH31
LH11	LH25	LH12	LH27	LH21	LH13	LH8

Fig. B.6. Optimal relay nodes for CHs or CLs.

ues of the corresponding vector's index are 0 and 1, respectively, as shown in Fig. B.3.

4) Performs a mutation function, utilizing the random resetting mutation method, among the children where, for example, the 4th gene of each new child (chromosome) is mutated based on the list {LH8, LH25, LH27, LH9} taking into consideration the selection of one entry at a time in order, as shown in Fig. B.4.
5) Conducts another crossover function between the parents which is similar to the that performed earlier, as shown in Fig. B.5.
6) Obtains the optimal relay node for each CH after performing genes' mutation, similar to that performed in step 4, as shown in Fig. B.6.

CRediT authorship contribution statement

Khalid A. Darabkh: Conceptualization, Methodology, Formal analysis, Investigation, Validation, Writing - review & editing. **Wafa'a K. Kassab:** Conceptualization, Methodology, Formal analysis, Investigation, Validation, Writing - review & editing. **Ala' F. Khalifeh:** Conceptualization, Methodology, Formal analysis, Investigation, Validation, Writing - review & editing.

References

[1] R. Prasad, V. Rohokale, Internet of Things (IoT) and Machine to Machine (M2M) Communication, Cyber Security: the Lifeline of Information and Communication Technology, Springer Series in Wireless Technology, Cham, Switzerland, 2020, pp. 125–141. Chapter 9.

[2] W. Kassab, K. Darabkh, A-Z survey of internet of things: architectures, protocols, applications, recent advances, future directions and recommendations, J. Netw. Comput. Appl. 163 (2020) 102663.

[3] L. Atzori, A. Iera, G. Morabito, Understanding the Internet of Things: definition, potentials, and societal role of a fast evolving paradigm, Ad Hoc Netw. 56 (2017) 122–140.

[4] L. Xu, R. Collier, G. OHare, A survey of clustering techniques in WSNs and consideration of the challenges of applying Such to 5G IoT scenarios, IEEE Internet Things J. 4 (5) (2017) 1229–1249.

[5] K. Darabkh, M. Judeh, H. Bany-Salameh, S. Althunibat, Mobility aware and dual phase AODV protocol with adaptive hello messages over vehicular adhoc networks, AEU - Int. J. Electron. Commun. 94 (2018) 277–292.

[6] K. Darabkh, M. Alfawares, S. Althunibat, MDRMA: Multi-data rate mobility-aware AODV-based protocol for flying ad-hoc networks, Veh. Commun. 18 (2019).

[7] K. Darabkh, O. Alsukour, Novel protocols for improving the performance of ODMRP and EODMRP over mobile ad hoc networks, Int. J. Distrib. Sen. Netw. (IJDSN) 11 (10) (2015).

[8] Q. Li, S. Gochhayat, M. Conti, F. Liu, EnergIoT: A solution to improve network lifetime of IoT devices, Pervasive Mob. Comput. 42 (2017) 124–133.

[9] K. Darabkh, R. Muqat, An efficient protocol for minimizing long-distance communications over wireless sensor networks, International Multi-Conference on Systems, Signals & Devices (SSD), 2018.

[10] K. Darabkh, J. Zomot, Z. Al-qudah, EDB-CHS-BOF: energy and distance based cluster head selection with balanced objective function protocol, IET Commun. Spec. Issue 13 (19) (2019) 3168–3180.

[11] Y.-S. Jeong, Y.-H. Park, C.-H. Hsu, J. Park, A data aggregation based efficient clustering scheme in underwater wireless sensor networks, Ubiquitous Information Technologies and Applications, Springer, Berlin, Heidelberg, 2014.

[12] J. Long, O. Büyüköztürk, Collaborative duty cycling strategies in energy harvesting sensor networks, Comput. Aided Civ. Infrastruct. Eng. (2019).

[13] K. Darabkh, M. El-Yabroudi, A. El-Mousa, BPA-CRP: a balanced power-aware clustering and routing protocol for wireless sensor networks, Ad Hoc Netw. 82 (2019) 155–171.

[14] R. Al-Zubi, N. Abedsalam, A. Atieh, K. Darabkh, LBCH: load balancing cluster head protocol, Informatica 29 (4) (2018) 633–650.

[15] O. Younis, M. Krunz, S. Ramasubramanian, Node clustering in wireless sensor networks: recent developments and deployment challenges, IEEE Netw. 20 (3) (2006) 20–25.

[16] K. Darabkh, L. Al-Jdayeh, A New Fixed Clustering based algorithm for wireless sensor networks, International Wireless Communications & Mobile Computing Conference (IWCMC), 2018.

[17] K. Darabkh, W. Al-Rawashdeh, R. Al-Zubi, S. Alnabelsi, C-DTB-CHR: centralized density- and threshold-based cluster head replacement protocols for wireless sensor networks, J. Supercomput. 73 (12) (2017) 5332–5353.

[18] K. Darabkh, N. Maaitah, I. Jafar, A. Khalifeh, Energy Efficient Clustering Algorithm for Wireless Sensor Networks, International Conference on Wireless Communications, Signal Processing and Networking (WiSPNET), 2017.

[19] K. Darabkh, W. Kassab, A. Khalifeh, Maximizing the Life Time of Wireless Sensor Networks Over IoT Environment, In proceedings of the Sixth International Workshop on Internet of Things: Networking Applications and Technologies (IoTNAT 2020) in conjunction with 5th IEEE International Conference on Fog and Mobile Edge Computing (FMEC 2020), 2020.

[20] H. Li, Y. Liu, W. Chen, W. Jia, B. Li, J. Xiong, COCA: Constructing optimal clustering architecture to maximize sensor network lifetime, Comput. Commun. 36 (3) (2013).

[21] K. Darabkh, S. Odetallah, Z. Al-qudah, A. Khalifeh, M. Shurman, Energy–aware and density-based clustering and relaying protocol (EA-DB-CRP) for gathering data in wireless sensor networks, Appl. Soft Comput. 80 (2019) 154–166.
[22] K. Darabkh, L. Al-Jdayeh, AEA-FCP: an adaptive energy-aware fixed clustering protocol for data dissemination in wireless sensor networks, Pers. Ubiquitous Comput. (2019) 1–19.
[23] T. Liu, Q. Li, P. Liang, An energy-balancing clustering approach for gradient-based routing in wireless sensor networks, Comput. Commun. 35 (17) (2012) 2150–2161.
[24] Y. Guo, Y. Liu, Z. Zhang, F. Ding, Study on the energy efficiency based on improved LEACH in wireless sensor networks, International Asia Conference on Informatics in Control, Automation and Robotics, 2010.
[25] D.-h. Nam, H.-k. Min, An Energy-Efficient Clustering Using a Round-Robin Method in a Wireless Sensor Network, International Conference on Software Engineering Research, Management and Applications, 2007.
[26] J. Hong, J. Kook, S. Lee, D. Kwon, S. Yi, The method of threshold-based cluster head replacement for wireless sensor networks, Inf. Syst. Front. 11 (5) (2009).
[27] F. Zhao, Y. Xu, R. Li, Improved LEACH Routing Communication Protocol for a Wireless Sensor Network, Int. J. Distrib. Sens. Netw. 8 (12) (2012).
[28] G. Chen, C. Li, M. Ye, J. Wu, An unequal cluster-based routing protocol in wireless sensor networks, Wirel. Netw. 15 (2) (2009).
[29] K. Darabkh, N. Al-Maaitah, I. Jafar, A. Khalifeh, EA-CRP: a novel energy-aware clustering and routing protocol in wireless sensor networks, Comput. Electr. Eng. 72 (2018) 702–718.
[30] K. Darabkh, J. Zomot, Z. Al-qudah, A. Khalifeh, IEDB-CHS-BOF: improved energy and distance based CH selection with balanced objective function for wireless sensor networks, In proceedings of the Sixth International Workshop on Internet of Things: Networking Applications and Technologies (IoTNAT 2020) in conjunction with 5th IEEE International Conference on Fog and Mobile Edge Computing (FMEC 2020), 2020.
[31] K. Darabkh, N. Alsaraireh, A yet efficient target tracking algorithm in wireless sensor networks, IEEE 2018 15th International Multi-Conference on Systems, Signals & Devices (SSD), 2018.
[32] K. Darabkh, M. EL-Yabroudi, A Reliable Relaying Protocol in Wireless Sensor Networks, IEEE 2017 European Conference on Electrical Engineering and Computer Science (EECS), 2017.
[33] K. Darabkh, S. Odetallah, Z. Al-qudah, A. Khalifeh, A new density-based relaying protocol for wireless sensor networks, IEEE 2018 14th International Wireless Communications & Mobile Computing Conference (IWCMC), 2018.
[34] K. Darabkh, J. Zomot, An improved cluster head selection algorithm for wireless sensor networks, IEEE 2018 14th International Wireless Communications & Mobile Computing Conference (IWCMC), 2018.
[35] K. Darabkh, S. Ismail, M. Al-Shurman, I. Jafar, E. Alkhader, M. Al-Mistarihi, Performance evaluation of selective and adaptive heads clustering algorithms over wireless sensor networks, J. Netw. Comput. Appl. 35 (6) (2012).
[36] M. Shankar, R. Singh, Performance evaluation of LEACH protocol in wireless network, Int. J. Sci. Eng. Res. 3 (1) (2012).
[37] K. Darabkh, W. Al-Rawashdeh, M. Hawa, R. Saifan, MT-CHR: a modified threshold-based cluster head replacement protocol for wireless sensor networks, Comput. Electr. Eng. 72 (2018) 926–938.
[38] K. Darabkh, W. Albtoush, I. Jafar, Improved clustering algorithms for target tracking in wireless sensor networks, J. Supercomput. 73 (5) (2017) 1952–1977.
[39] H. Majid, K. Abdul Rahim, R. Hamid, A. Murad, F. Ismail, Frequency-reconfigurable microstrip patch-slot antenna, IEEE Antennas Wirel. Propag. Lett. 12 (2013) 218–220.
[40] S. Ullah, S. Ahmad, B. Khan, J. Flint, A multi-band switchable antenna for Wi-Fi, 3G Advanced, WiMAX, and WLAN wireless applications, Int. J. Microwave Wireless Technol. 10 (8) (2018) 991–997.
[41] T. Saaty, Fundamentals of Decision Making and Priority Theory With the Analytic Hierarchy Process, McGraw Hill, New York, 2000.
[42] Y. Chou, C. Lee, J. Chung, Understanding m-commerce payment systems through the analytic hierarchy process, J. Bus. Res. 57 (12) (2004).
[43] S. Hamblin, T. Hansen, On the practical usage of genetic algorithms in ecology and evolution, Methods Ecol. Evol. 4 (2) (2013).
[44] N. Soni, T. Kumar, Study of various mutation operators in genetic, Int. J. Comput. Sci. Inf. Technol. 5 (2014) 4519–4521.
[45] F. Behrouz, C. Sophia, Data Communications and Networking, 4th Edition, McGraw-Hill, New York, 2007.
[46] P. Elejoste, I. Angulo, A. Perallos, A. Chertudi, I. Zuazola, A. Moreno, L. Azpilicueta, J. Astrain, F. Falcone, J. Villadangos, An easy to deploy street light control system based on wireless communication and LED technology, Sensors 13 (5) (2013).
[47] J. Jang, H. Kim, H. Cho, Smart roadside system for driver assistance and safety warnings: framework and applications, Sensors 11 (12) (2011).
[48] W. Du, Z. Xing, M. Li, B. He, C. Chua, H. Miao, Optimal sensor placement and measurement of wind for water quality studies in urban reservoirs, in: IPSN-14 Proceedings of the 13th International Symposium on Information Processing in Sensor Networks, Berlin, 2014.
[49] M. Rao, G. Anandakumar, Optimal placement of sensors for structural system identification and health monitoring using a hybrid swarm intelligence technique, Smart Mater. Struct. 16 (6) (2007).
[50] K. Sattlegger, U. Denk, Navigating your Way through the RFID Jungle, 2014 Texas Instruments white paper.
[51] P. Sethi, S.R. Sarangi, Internet of Things: architectures, protocols, and applications, Hindawi J. Electr. Comput. Eng. 2017 (2017) 1–25.
[52] "Mass scale smart city technology," [Online]. Available: https://www.telensa.com/. [Accessed 25 July 2019].
[53] K. Mekki, E. Bajic, F. Chaxel, F. Meyer, A comparative study of LPWAN technologies for large-scale IoT deployment, ICT Express 5 (1) (2019) 1–7.
[54] "What is the LoRaWAN® Specification?," [Online]. Available: https://lora-alliance.org/about-lorawan. [Accessed 15 July 2019].

Khalid A. Darabkh Received the PhD degree in Computer Engineering from the University of Alabama in Huntsville, USA, in 2007 with honors. He has joined the Computer Engineering Department at the University of Jordan as an Assistant Professor since 2007 and has been a Tenured Full Professor since 2016. He is engaged in research mainly on wireless sensor networks, mobile-ad hoc networks, vehicular networks, flying ad hoc networks, queuing systems and networks, multimedia transmission, Internet of things, cognitive radio networks, channel coding, steganography and watermarking, as well as innovative and interactive learning environments. He authored and co-authored of at least a hundred forty research articles and served as a reviewer in many scientific journals and international conferences. Prof. Darabkh is the recipient of 2016 Ali Mango Distinguished Researcher Reward for Scientific Colleges and Research Centers in Jordan. He is further the recipient of the University of Jordan's appreciation certificate as of being the researcher who publish the highest number of quality manuscripts in Scopus during 2018. As far as software certifications tracks are concerned, he is Sun Certified Programmer for Java Platform (SCJP), Oracle Database Administrator Certified Associate (OCA), as well as Oracle Java Developer Certified Trainer (OJDC-T). In fact, he serves on the Editorial Board of Telecommunication Systems, published by Springer, Computer Applications in Engineering Education, published by John Wiley & Sons, and Journal of High Speed Networks, published by IOS Press. Additionally, he serves as a TPC member of highly reputable IEEE conferences such as GLOBECOM, LCN, VTC-Fall, PIMRC, ISWCS, ATC, ICT, and IAEAC. Moreover, he is a member of many professional and honorary societies, including Eta Kappa Nu, Tau Beta Pi, Phi Kappa Phi, and Sigma XI. He was selected for inclusion in the Who's Who Among Students in American Universities and Colleges and Marquis Who's Who in the World. As administrative experience at the University of Jordan, he served as Assistant Dean for Computer Affairs in the College of Engineering from Sept 2008 to Sept 2010. Additionally, he served as Acting Head of the Computer Engineering Department from June 2010 to Sept 2012.

Wafa'a Kassab received the B.Sc. degree in computer engineering from Al-Balqa' Applied University, Amman, Jordan, in 2011. She received further her M.Sc. degree in computer engineering and networks from the University of Jordan, Amman, Jordan, in 2018. Her research interests include wireless networks, sensor networks, and Internet of Things.

Ala' Khalifeh received the PhD degree in Electrical and Computer Engineering from the University of California, Irvine - USA in 2010. He is currently an Associate Professor in the Communication Engineering department at the German Jordanian University and the department chair. His research is in communications technology, and networking with particular emphasis on optimal resource allocations for multimedia transmission over wired and wireless networks, Quality of Service, Internet of Things and Wireless Sensor Networks.